Ecological Indicators 150 (2023) 110206

Contents lists available at ScienceDirect

Ecological Indicators

journal homepage: www.elsevier.com/locate/ecolind

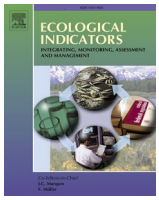

Original Articles

Spatiotemporal variation characteristics of sediment nutrient load from the soil erosion of the Yangtze River Basin of China from 1901 to 2010

Xixi Liu [a,b], Yufei Bao [a,b], Yuchun Wang [a,b,*], Di Zhang [d], Mingming Hu [a,b], Xinghua Wu [c], Jie Wen [a,b], Shanze Li [a,b], Meng Sun [d]

[a] State Key Laboratory of Simulation and Regulation of Water Cycle in River Basin, China Institute of Water Resources and Hydropower Research, Beijing 100038, China
[b] Department of Water Ecology and Environment, China Institute of Water Resources and Hydropower Research, Beijing 100038, China
[c] Ecological Environment Engineering Research Center of the Yangtze River, China Three Gorges Corporation, Beijing 100038, China
[d] Institute of Earth Sciences, China University of Geosciences, Beijing, Beijing 100038, China

ARTICLE INFO

Keywords:
Yangtze River Basin
Soil erosion
Absorbed nitrogen
Absorbed phosphorous
Nutrient loss empirical model (NLEM)
Revised universal soil loss equation (RUSLE)
Sediment load

ABSTRACT

Over the past 70 years, the Yangtze River Basin-the third longest river basin in the world-has been under the influence of augmented human activities. Regarding environmental protection and policy design, the total nitrogen and phosphorus (TN and TP, respectively) loads from soil erosion are objectively and quantitatively critical parameters while assessing the spatio-temporal soil erosion changes over the 1901–2010 period. First, soil erosion in our study area was calculated using the Revised Universal Soil Loss Equation (RUSLE) model. Second, the TN and TP loads from soil erosion were assessed using the constructed Nutrient Loss Empirical Model (NLEM). Third, we conducted spatial autocorrelation analysis, Mann-Kendall (M–K) trend tests, and wavelet analysis of the soil erosion, and related TN and TP loads. At Datong Station over the 1901–2010 period, the average annual TN and TP loads from soil erosion were 1.77 and 0.56 million tonnes, respectively. Moran's I values of the average annual soil erosion, and related TN and TP loads from soil erosion indicates the existence of positive correlations, while clustering was the prevailing spatial distribution pattern. High-high (H-H) cluster areas were mainly evident in high-altitude region of the western and southern Yangtze River Basin, conversely, low-low (L-L) cluster areas were scattered primarily in regions with high population density and intense human activities. Soil erosion increased rapidly around 2001; hence, 2001 was a changing point. According to the M–K test, the time intersection of soil erosion, and related TN and TP loads at Datong Station was around 1990; hence, 1990 may have been a changing point, likely due to the operation of Gezhouba Dam during 1981-1986. This Dam trapped large amounts of sediments. If the sediment load data of control hydrological station of 12 sub-basins is available, SDR, sediment load, AN and AP calculation could be more accurate and interpretable.

1. Introduction

Yangtze River is the longest river in China and Asia and third longest river in the world; as it flows across China from west to east, its basin crosses Qinghai, Tibet, Sichuan, Yunan, Chongqing, Hunan, Hubei, Jiangxi, Anhui, Jiangsu and Shanghai (Wang et al., 2019a; Wang et al., 2019ab). The Yangtze River Basin comprises an area of 1.8 million km^2, covering 18% of the total area of China (Qu et al., 2020). Therefore, its water resource endowment ranks first in the world (Penghao et al., 2019).

According to historical data, the period before 1968 is the pre-dam construction time in the Yangtze River Basin (Yang et al., 2018). Most of the river sediment is retained by dams, with research suggesting that the Three Gorges Dam retains 80% of the upstream sediment (Yang et al., 2018). Sediment concentration decreases along the basin because the impact of water discharge is small. The two main factors contributing to sediment loss in the basin are precipitation intensity and sediment delivery ratio (SDR) (Wu et al., 2013). The increased construction of hydropower stations in this area resulted in highly controversial problems, for example regarding the nutrient balance conditions in the basin becoming prominent (Zhou et al., 2008; Tong et al., 2017; Strokal et al., 2020; Li et al., 2022; Zhao et al., 2022). Hydropower stations trap sediments and nutrients within the basin, thereby affecting downstream areas, such as wetlands, fisheries and agricultural areas (Lanza, 2011).

* Correspondence author at: Department of Water Ecology and Environment, China Institute of Water Resources and Hydropower Research, Beijing 100038, China.
E-mail address: wangyciwhr@163.com (Y. Wang).

https://doi.org/10.1016/j.ecolind.2023.110206
Received 6 December 2022; Received in revised form 28 March 2023; Accepted 29 March 2023
Available online 6 April 2023

Between 2000 and 2010, there were more than 500 major harmful algal blooms incidents related to excessive nitrogen in the Yangtze River Estuary and adjacent waters (Shen et al., 2011). In recent 10 years, the water quality of Yangtze River Basin has improved significantly, but local water pollution is still serious and has not been effectively controlled. For example, the water quality of some rivers and tributaries along the main stream cities is relatively poor, and some lakes are suffering from serious eutrophication, and the water quality safety of some water sources is insufficient, thus increasing the potential risk of water pollution. The total nitrogen and phosphorus (TN and TP, respectively) loads can be classified into dissolved and absorbed nitrogen and phosphorous (DN, AN and DP, AP, respectively). Soil can be regarded as migration carrier of AN and AP. Nitrogen and phosphorous are absorbed by sediments and subsequently enter the water stream (Zhang et al., 2020a). In accordance with the surface water quality standard of China (GB3838-2002), water samples should settle for 30 min after collection and the non-settled part of the upper layer should be analysed according to the prescribed method (Wang et al., 2016). Consequently, without the sediment content in the water sample, estimating the AN and AP carried by sediment is not possible. Research suggested that in the Lancang River Basin, the TP load from soil erosion accounts for 69% of the TP load in the basin (Zhang et al., 2020a). In addition, during the rainy season in the Yangtze downstream area, the proportion of particulate phosphorus (PP) in TP is approximately 93% (Dong et al., 2020). Nitrogen and phosphorus are important biogenic substances, hence, the TN and TP loads from soil erosion entering Yangtze River require accurate estimations.

Datong Station lacks sediment load data before 1953, while, data of the TN and TP loads from soil erosion are also missing. AN and AP originate mainly from soil erosion, especially in large basins (Zhang et al., 2020a). Soil erosion models began to develop since 1960s (Fang et al., 2019). It is an effective tool for modeling soil loss. Physical processes and conceptual models have been studied and acquired creative results, such as, universal soil loss equation (USLE), revised universal soil loss equation (RUSLE), physical model, water erosion prediction project (WEPP), and distributed model (Cilek et al., 2015; Kinnell, 2017; Mirzaee et al., 2017; Sonnenborg et al., 2017). In these models, practicable USLE and RUSLE have been widely applied for soil erosion estimation (Wischmeier and Smith, 1978). These two models took factors which affecting soil erosion into account in the estimation process. University faculty and federal scientists across the USA conducted decades of soil erosion experiments and developed USLE in the twentieth century. USLE model was mainly applied for the soil erosion of areas of croplands or gentle slope topography. RUSLE model is the revised version of USLE model (Ganasri and Ramesh, 2016). RUSLE and Geographic Information System (GIS) technique were applied together to predict the soil erosion in the Nethravathi Basin and Kasai River Basin, India (Alewell et al., 2008; Wischmeier and Smith, 1978). RULSE and NLEM model has been applied in Lancang River to model soil erosion and TP load from soil erosion (Zhang et al., 2020a). Although there are many problems in soil erosion model simulation because the mechanism of soil erosion occurrence and development is not very clear, it is still an effective method to evaluate the temporal and spatial evolution of soil erosion. There are few simulation assessments of centennial soil erosion estimation. There are two types of models available for the calculation of the TN and TP loads, namely empirical models and physical based models. Physically based models, such as the Soil and Water Assessment Tool (SWAT) are advantageous since they can model the natural nitrogen and phosphorus with higher veracity, however, calibrations and simulations require high-quality spatially distributed data. Empirical models, such as the Nutrient Loss Empirical Model (NLEM), can estimate the AN and AP loads even when the data are limited, however, the acceptable accuracies are based on experience (Zhang et al., 2020a). NLEM has been applied on the worldwide watershed, such as, River Raisin, the Burdekin River Basin, and Luan River Watershed and has been validated that NLEM is a feasible and reasonable method to simulate nutrient loss (Tao et al., 2010). AP load of Lancang River has been calculated based on the NLEM, whereas, the phosphorus content in soil used in this model was the average background content of phosphorus on each type of soil from different monitoring sites due to the lack of spatial distribution data (Zhang et al., 2020a). Nevertheless, the theoretical foundation of the NLEM is based on a physically based model. Considering the limited monitoring data, in this paper, the Revised Universal Soil Loss Equation (RUSLE) model was employed to calculate soil erosion over the 1901–2010 period. In addition, Nutrient Loss Empirical Model (NLEM) was applied for the calculation of TN and TP loads from soil erosion.

In this study, the authors (1) focused on the calculation of soil erosion in the Yangtze River Basin during the period of 1901–2010, (2) simulated the TN and TP loads from soil erosion in the Yangtze River Basin from 1901 to 2010, (3) examined the spatio-temporal variations of soil erosion, and AN and AP loads in the Yangtze River Basin. As the construction of dams in the Yangtze River Basin, this research hypothesis variation trend of the sediment load at Datong station and AN and AP value would decrease as dam would trap large amount of sediment.

2. Method

2.1. Study region

The area and length of the Yangtze River Basin are 1.8 million km^2 and >6300 m respectively (Penghao et al., 2019). The Yangtze River Basin is divided into three subsections, namely the upper, middle and lower reaches (Xi et al., 2017). The upper, middle and lower reaches of the Yangtze River Basin extend from its source to Yichang, from Yichang to Hukou and from Hukou to Datong, respectively (Wang et al., 2019a; Wang et al., 2019b). The region is characterized by subtropical monsoon climate, with the mean annual precipitation being about 1100 mm (Penghao et al., 2019). The Yangtze River Basin (Fig. 1) can be divided into 12 sub-basins, namely Jinsha River above the Shigu basin (S1), Jinsha River below the Shigu basin (S2), mainstream from Yibin to Yichang (S3), mainstream from Yichang to Hukou (S4), mainstream below Hukou (S5), Taihu Lake basin (S6), Min-Tuo River basin (S7), Jialing River basin (S8), Hanjiang River basin (S9), Wujiang River basin (S10), Dongting Lake basin (S11) and Poyang Lake basin (S12).

As the mother river and an important producing area for high quality sand mining in China, >400 million people were supported by Yangtze River and there were >50,000 dams have been built by 2010 in the Yangtze River Basin since 1950s (Yang et al., 2005). Environmental and ecological issues including water chemistry changes occurred as the operation of Three Gorges Dam (TGD). The upper reaches of this basin is the contributing sediment area to the East China Sea. Large amounts of sediments would be trapped by the Dam and give rise to the significantly sediment decrease. Datong Station is the control station of the Yangtze River Basin. Presently, the sediment load is not available before 1953 in Datong station. Algal blooms accidents occurred in the YRB associated with excessive nitrogen and phosphorus levels in the YRB and adjacent areas (Zhang et al., 2021). Yangtze estuary is one of the most contaminated areas in China, and eutrophication has received increasing attention. Mississippi River which is also great river faces the same issue (Alexander et al., 2009). Lancang River is also facing the ecosystem deterioration condition. Besides, there is a lack of scientific estimation of absorbed nitrogen and phosphorus carried by sediment. On account of dam construction, the sediment load and nutrient balance become a highly disputed issues in the Yangtze River Basin (Guo and Li, 2003; Tong et al., 2017).

2.2. Data sources and processing

The value of L, S, K and $C_{N/P}$ in soil are same from 1901 to 2010 as the DEM, soil types and soil properties of Yangtze River Basin could be regarded as invariant. Datasets with different spatial resolution were

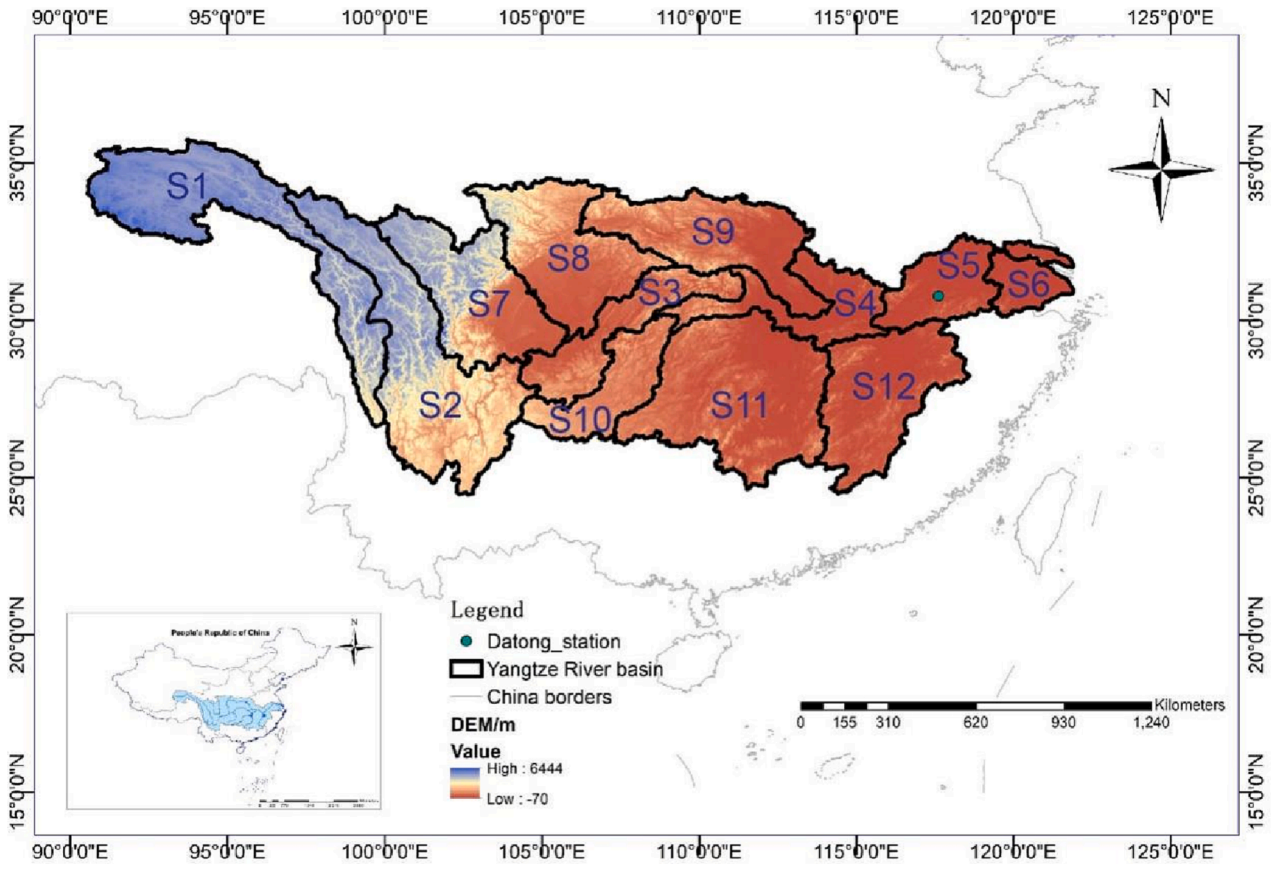

Fig. 1. The Yangtze River basin Basin image and its 12 sub-basins, namely Jinsha River above the Shigu basin (S1), Jinsha River below the Shigu basin (S2), mainstream from Yibin to Yichang (S3), mainstream from Yichang to Hukou (S4), mainstream below Hukou (S5), Taihu Lake basin (S6), Min-Tuo River basin (S7), Jialing River basin (S8), Hanjiang River basin (S9), Wujiang River basin (S10), Dongting Lake basin (S11) and Poyang Lake basin (S12).

resampled to the uniform spatial resolution of 1 km using 'Resample' tool in the ArcToolbox of Arcmap software. This is because when grid merging, spatial analysis must specify the pixel of the input grid for each output pixel, and this specification process is called resampling.

The data and main parameters used in this research are listed in Table 1. The monthly precipitation dataset was obtained from National Tibetan Plateau Data Center (https://data.tpdc.ac.cn/en/). The time range and spatial resolution of it are 1901.1–2010.12 and 1 km. The Arcmap software was used for format conversion, 'define projection' to get WGS1984 coordinate system and clip of the data to get the monthly 1 km precipitation dataset of Yangtze River Basin. Monthly precipitation dataset was applied to calculate the rainfall erosivity factor (R). The temporal resolution of R would be years from 1901 to 2010.

National DEM 1 km data was downloaded from Resource and Environment Science and Data Center (https://www.resdc.cn/). The coordinate system is WGS 1984. The Arcmap software was applied for 'clip' tool to get the study region, 'slope' tool to get slope angle (θ) for factor S calculation. Regarding factor L, 'Fill', 'Flow Direction', and 'Flow Accumulation' hydrology tool in Arcmap software was utilized to get flow accumulation for factor L calculation. It was applied to get the slope length factor (L) and slope steepness factor (S) in the RUSLE model.

Soil erosivity factor (K) whose spatial resolution is 30 m was applied

Table 1
Data sources.

Dataset	Period	Temporal resolution	Spatial resolution	Data sources
1-km monthly precipitation dataset for China (Ding and Peng, 2020; Peng, 2020; Peng et al., 2019, 2018, 2017).	1901–2010	monthly	1 km	National Tibetan Plateau Data Center (https://data.tpdc.ac.cn/en/)
National digital elevation models (DEM) at 1 km, 500 m and 250 m resolutions (SRTM 90 M)			1 km	Resource and Environment Science and Data Center (https://www.resdc.cn/)
Soil erodibility factor (K)	2018		30 m	National Earth System Science Data Center, National Science & Technology Infrastructure of China (https://www.geodata.cn)
Spatial distribution of annual 1 km normalized difference vegetation index (NDVI) for China	1998–2010	annual	1 km	Resource and Environment Science and Data Center (https://www.resdc.cn/)
Remotely sensed land use status for China	1990,1995,2000,2005,2010	annual	1 km	Resource and Environment Science and Data Center (https://www.resdc.cn/)
Soil properties for land surface modelling over China (Shangguan et al., 2013)			30 arcseconds	National Tibetan Plateau Data Center (https://data.tpdc.ac.cn/en/)
Sediment load data from Datong Station (2010 Yangtze River Sediment Bulletin)	1953–2010	annual		Changjiang Water Resources Commission of the Ministry of Water Resources (https://www.cjw.gov.cn/)

from National Earth System Science Data Center, National Science & Technology Infrastructure of China (http://www.geodata.cn) to calculate soil erosion. Different soil types are assigned different K values (Beskow et al., 2009). The coordinate system is WGS 1984. The Arcmap software was used for 'clip' tool to get the study region and 'resample' tool to uniform the spatial resolution to 1 km.

Annual NDVI data from 1998 to 2010 were employed to figure out the vegetation cover and management factor (C). The time series dataset was downloaded from Resource and Environment Science and Data Center (https://www.resdc.cn/). The spatial resolution is 1 km. 'Clip' tool in Arcmap software was applied to get the study region raster data. As many studies indicated that the soil erosion rate in the basin is more sensitive to rainfall and data missing (Dabral et al., 2008; Jain et al., 2001). The major force in Yangtze River behind soil erosion is precipitation (Wang et al., 2011). On account of NDVI data before 1998 is unavailable, C value before 1998 were replaced by C value in 1998.

1990, 1995, 2000, 2005 and 2010 remote sensing monitoring database of land use status were obtained from Resource and Environment Science and Data Center (https://www.resdc.cn/). These data were applied to get the conservation practice factor (P). The spatial resolution is 1 km. 'Clip' tool in Arcmap software was used to get the Yangtze River Basin raster data. As the land use data before 1990 is missing, annual P value from 1901 to 1989 were replaced by land use data in 1990 because the expansion rate dramatically increased period time of Yangtze River Basin was from 2006 to 2013 during which number of cities and urban built-up area generally added (Zhong et al., 2020). The value of P in 1991 and 1992 were replaced by 1990 and the value of 1993 and 1994 were replaced by 1995 because the land use type data is available every five years, and so on, the P value for subsequent years were also calculated in accordance with this rule.

Dataset of soil properties for land surface modeling over China was obtained from National Tibetan Plateau Data Center (http://data.tpdc.ac.cn/en/). These datasets contain $C_{N/P}$ (total nitrogen or phosphorus content (%, g/100 g)) in the soil which could be applied for TN and TP load from soil erosion calculation by Nutrient Losses Empirical Model (NLEM). The coordinate system is WGS 1984. The Arcmap software was used for 'clip' tool to get the study region and 'resample' tool to uniform the spatial resolution to 1 km.

2.3. Methodology

2.3.1. TN and TP loads from soil erosion

The NLEM was applied and 'Raster calculator' tool in Arcmap software was applied to model the TN and TP loads from natural soil erosion (Ding et al., 2017). The equation is expressed as follows:

$$L_{SE} = Q_S \bullet C_{N/P} \bullet \eta$$

where Q_S is the sediment entering the study basin annually, $C_{N/P}$ is the TN or TP content (%, g/100 g) in soil and η represents the soil enrichment ratio of AN and AP (dimensionless). The value of η is 1.77 (Wang et al., 2015a; Wang et al., 2015b).

2.3.2. Sediment entering into the river

The sediment entering the river is calculated as follows:

$$Q_S = X \bullet \mathrm{SDR}$$

where X represents soil erosion and SDR is the sediment delivery ratio (dimensionless).

2.3.3. Sediment delivery ratio (SDR)

Sediment load data from Datong Station covering the 1953–2010 period were retrieved from the 2010 Yangtze River bulletin. As sediment from soil erosion is trapped by dams, it is necessary to remove the effect of dams on sediment when calculating the SDR. The period before 1968 is the pre-dam construction time in the Yangtze River Basin (Yang et al., 2018).

SDR is the ratio of sediment entering the river to the natural soil erosion (Zhang et al., 2020a). The equation of it is as follows:

$$SDR = \bar{Q}_S/(A_S \bullet X_y)$$

where $\bar{Q}_S$ is the average annual sediment transport into the Yangtze River Basin measured at Datong Station during 1953–1968, A_s is the watershed control area at Datong Station and X_y is the average annual soil erosion of the Yangtze River Basin during 1953–1968. The calculated SDR during 1953–1968 was found to be 0.16. For extending the Datong Station dataset back to 1901–1952, calculated SDR was applied and the sediment load was reconstructed.

2.3.4. Soil erosion

The RUSLE was utilised to quantify the natural soil erosion and 'Raster calculator' tool in Arcmap software was applied in the Yangtze River Basin (Wischmeier and Smith, 1978). The equation is as follows:

$$X = R \bullet K \bullet LS \bullet C \bullet P$$

where X is the average value of soil loss or erosion ($t{\cdot}ha^{-1}{\cdot}a^{-1}$), R is the rainfall erosivity factor ($MJ{\cdot}mm{\cdot}ha^{-1}{\cdot}h^{-1}{\cdot}a^{-1}$), K is the soil erosivity factor ($t{\cdot}ha{\cdot}h{\cdot}ha^{-1}{\cdot}MJ^{-1}{\cdot}mm^{-1}$), L is the slope length factor (dimensionless), S is the slope steepness factor (dimensionless), C is the vegetation cover and management factor (dimensionless), and P is the conservation practice factor (dimensionless) (Fang et al., 2019).

R is expressed as follows (Wischmeier and Smith, 1978):

$$R = \sum_{i=1}^{12} (-1.15527 + 1.792P_i)$$

where P_i is monthly rainfall (mm).

L is expressed as follows (Thomas et al., 2018):

$$L = (\frac{\lambda}{22.1})^m$$

where λ is the slope length (m) which is the product of flow accumulation and cell size of the dataset, m is the slope-length exponent (dimensionless), and θ is the slope angle (°). When $\theta > 5°$, m = 0.5, when $3.5° \le \theta \le 5°$, m = 0.4, when $1° \le \theta < 3.5°$, m = 0.3, and when $\theta < 1°$, m = 0.2. S is expressed as follows (Thomas et al., 2018):

$$S = \begin{cases} 10.8\sin\theta + 0.03, \theta < 5^{\circ} \\ 16.8\sin\theta - 0.5, 5^{\circ} < \theta < 10^{\circ} \\ 21.9\sin\theta - 0.96, \theta \ge 10^{\circ} \end{cases}$$

where θ represents the slope angle (°).

C is expressed as follows (Thomas et al., 2018; van der Knijff et al., 2000):

$$C = \frac{(-NDVI + 1)}{2}$$

where NDVI is the normalised difference vegetation index.

P is expressed as in Table 2 (Chuenchum et al., 2020; Yang et al., 2003):

2.3.5. Model calibration

Relative error was applied for the calibration of AP value modeled by NLEM model. The expression is shown as below:

Table 2
P factor values.

Land cover	Cropland	Forest	Grassland	Water body	Urban area	Unused land
P	0.5	0.9	0.9	0	1	1

$$D(\%) = 100^{*}\frac{Q_s - Q_0}{Q_0}$$

where D on behalf of the relative error, Q_s is the estimated value and Q_0 is the monitored value.

2.3.6. Spatial auto-correlation analysis

Spatial auto-correlation analysis was applied to assess soil erosion (X), and the TP and TN loads from natural soil erosion ($L_{SE\text{-}TP}$ and $L_{SE\text{-}TN}$, respectively). Global Moran's I was used to assess the global spatial auto-correlation and Local Moran's I was applied to assess the spatial association locally. Spatial auto-correlation is used for evaluating the distribution of spatial homogeneity of an ecological environment index within an area (Fan and Cowley, 1985). Average soil erosion (X), TP load from natural soil erosion ($L_{SE\text{-}TP}$) and TN load from natural soil erosion ($L_{SE\text{-}TN}$) maps from 1901 to 2010 were calculated and spatial auto-correlation analysis was employed Moran's I value ranges from −1 to 1. An absolute Moran's I value close to 1 indicates strong spatial correlation, while an absolute Moran's I value close to 0 indicates no spatial auto-correlation (Getis and Griffith, 1988). The correlation of each grid cell in the area of interest could be effectively expressed by Local Moran's I (LISA index) (Anselin, 1995). The local spatial aggregation of the LISA cluster map could be classified into five types, namely High-High (H-H) and Low-Low (L-L) clusters and Low-High (L-H) and High-Low (H-L) outliers, and no significant. An H-H cluster would indicate that both the selected grid unit and adjacent area values were high, whereas, an L-L cluster would indicate the exact opposite. An L-H outlier would indicate that the value of the selected grid unit was low, with the value of the adjacent area being high, whereas an H-L outlier would indicate the exact opposite. A no significant status would indicate the lack of a significant auto-correlation (Jing et al., 2020). The GeoDa software was employed for the Global Moran's I and Local Moran's I analyses.

2.3.7. Sequential T-test analysis of regime shift (STARS)

Sequential T-test analysis of regime shift (STARS) was performed to test the regime shifts of X, $L_{SE\text{-}TP}$, $L_{SE\text{-}TN}$ and rainfall time series, while employing the Sequential Regime Shift Detection software v3.2 in Excel environment, which is available the Bering Climate website (www.beringclimate.noaa.gov) (Rodionov, 2005).

2.3.8. Mann–Kendall trend test

Mann-Kendall trend tests of soil erosion, sediment load at Datong Station, TN and TP loads from soil erosion were conducted using the Matlab R2017a software (Zhang et al., 2006) The World Meteorological Organization recommends to applying this common method for assessing statistically significant trends of time series in hydro-meteorological datasets (Zhang et al., 2006). The sample sequence does not have to conform with a certain time distribution when using the M−K trend test. If the UF line changes within the critical line (95% confidence level), the variation tendency and regime shift of the changing indicator curve are not evident. If the value of UF is above 0, there is an increasing trend and vice versa. An intersection of the UF and UB lines within the critical line (95% confidence level) indicates a regime shift of the time series, however, if the intersection appears outside the critical line or multiple intersections are evident, other method are necessary to determine whether the intersections indicate regime shift.

2.3.9. Wavelet analysis

Wavelet analysis is usually performed for amplitude phase distribution detection at different frequencies (Torrence and Compo, 1998). Morlet wavelet analysis is a widely used method for identifying real-life oscillation periods (Duan et al., 2020). The Acycle v2.4.1 software was applied to conduct wavelet analysis of the time series of soil erosion sediment load at Datong Station and TN and TP loads from soil erosion in the Yangtze River Basin (Li et al., 2019).

3. Results

3.1. Validation and calibration for the proposed model

It has been verified that the NLEM is capable for modelling the sources of non-point contaminations at the upstream of Yangtze River (Ding et al., 2010, 2014; Shen et al., 2013). It has been demonstrated that sediment load verification can be used as basis for AP load validation because AP is mainly from soil erosion and the calculation of AP is based on soil erosion (Shen et al., 2013; Zhang et al., 2020a). Therefore, sediment discharge at Datong Station were used for the verification of absorbed nitrogen and absorbed phosphorus as these two indicators were calculated based on soil erosion (Shen et al., 2013). For AN (absorbed nitrogen) and AP (absorbed phosphorus) from soil erosion, there are only two AP monitored value for the Yangtze River Basin calibration (As shown in Table 3). In 2000, the relative error was −3.14% and in 2004, the relative error was −14.07% which indicating that the model was reasonable. As in 2004, the monitored data of AP was TP concentrations of the sediments in mean (g/kg). Besides, the sediment load in Datong station was calibrated by SDR. It could be assumed as the value of relative error from 1901 to 2010 floating between −14.07%. Datong Station was selected for this study as it is monitored and is representative of the entire basin (Yan et al., 2021). Over 95% of the sediment and water loads in Yangtze River is delivered above Datong Station, consequently, the nutrient fluxes at Datong Station approximate the totals over the entire basin (Duan et al., 2008; Zhiliang et al., 2003). Annual sediment loads at Datong Station for the 1953–2010 period were retrieved from the 2010 Yangtze River Sediment Bulletin. As stated previously, the period before 1968 is the pre-dam construction time in the Yangtze River Basin, hence, to remove effect of dams on the sediment load, SDR values for the 1953–1968 period were calculated by the ratio of the monitored sediment load at Datong Station and the annual soil erosion (Yang et al., 2018). Consequently, the SDR calculation process included the validation process of this model. Besides, the dataset of soil properties for land surface modelling over China was processed based on the Second National Survey, while focusing on the 1979–1985 period and surveying 2444 countries, 312 national farms and 44 forest farms in China (Shangguan et al., 2013). As a result, the TN and TP content uncertainties were not taken into consideration.

3.2. Spatial distribution

The average annual natural soil erosion of the Yangtze River Basin over the 1901–2010 period was 18.38 $t{\cdot}ha^{-1}{\cdot}a^{-1}$. The minimum and maximum values of natural soil erosion were 2.06 $t{\cdot}ha^{-1}{\cdot}a^{-1}$ in 1901 and 26.36 $t{\cdot}ha^{-1}{\cdot}a^{-1}$ in 1998 respectively. In particular, in 1901, the annual total precipitation was 243.3 mm, this was the minimum value over the 1901–2010 period and might have been the cause for the minimum natural soil erosion that year. In general, as illustrated in Fig. 2, higher soil erosion values were mainly distributed in the S1, S2 and S7 sub-basins of the Yangtze River Basin. The S1, S2 and S7 sub-basins are situated at higher elevations, comprising mountainous and hilly regions in the Yangtze River Basin (Alewell et al., 2008).

There are six classes of natural soil erosion: 0–5, 5–25, 25–50, 50–80, 80–150 and >150 $t{\cdot}ha^{-1}{\cdot}a^{-1}$ (Fang et al., 2019). For the average annual soil erosion during 1901–2010, the classes of 0–5, 5–25, 25–50, 50–80,

Table 3
The calibration of AP load in the Yangtze River Basin.

Year	Modeled AP load	Monitored AP load	Relative error	Units	Sources
2000	39.1	40.4	−3.14%	10,000 t	(Wang et al., 2011)
2004	0.6	0.8	−14.07%	g/kg	(Yang et al., 2017)

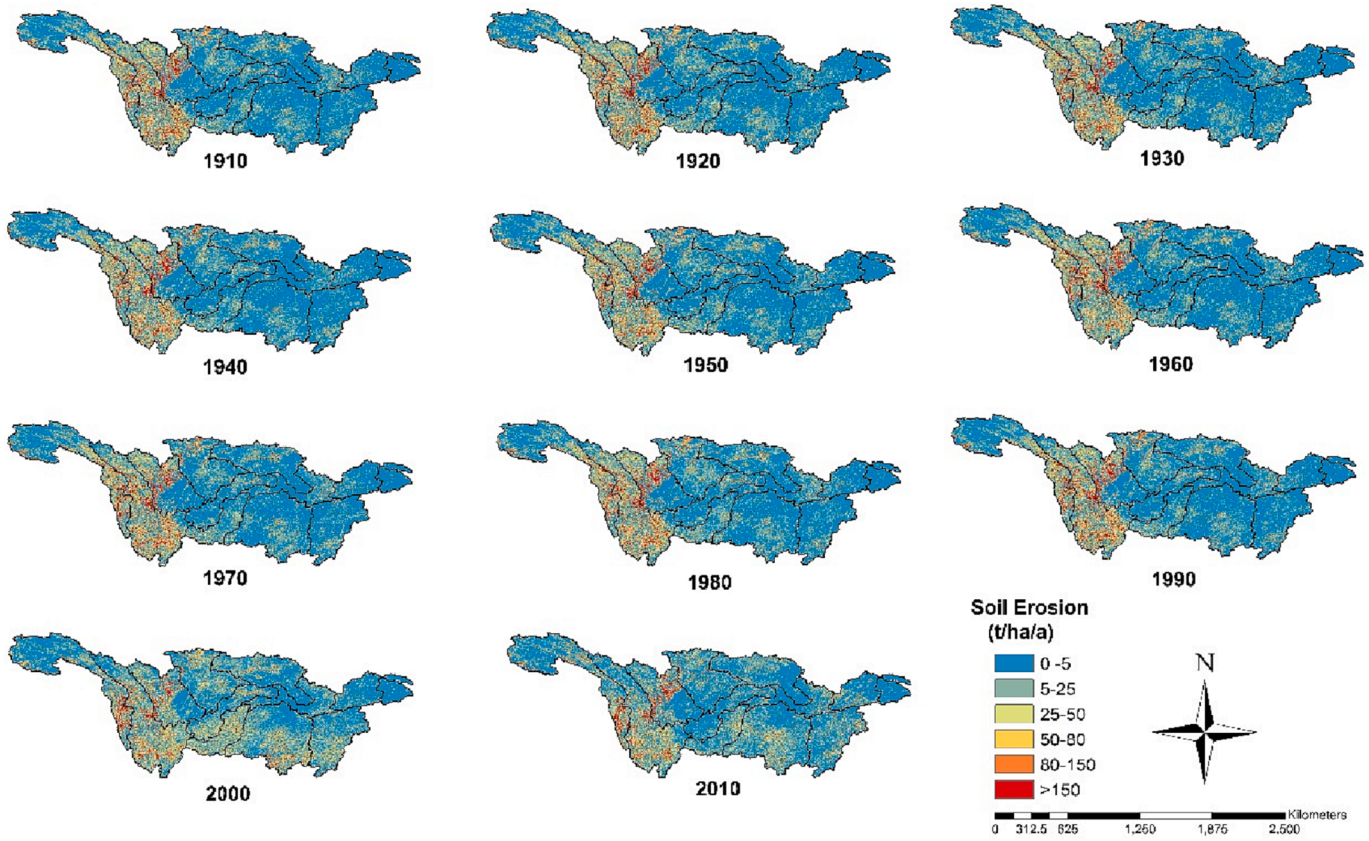

Fig. 2. Spatio-temporal variations of natural soil erosion in the Yangtze River Basin over the 1910–2010 period.

80–150 and > 150 t·ha^{-1}·a^{-1} of the Yangtze River Basin accounted for total areas of 38.74, 37.65, 10.76, 5.20, 4.41 and 3.23%, respectively (Table 4). Sub-basins S1, S2, S7 and S8 of the Yangtze River Basin belonged in the >150 t·ha^{-1}·a^{-1} soil erosion class. The >150 t·ha^{-1}·a^{-1} soil erosion class accounted for 10% of the total area of the S7 sub-basin.

The average annual TN load from soil erosion in the Yangtze River Basin over the 1901–2010 period was 0.01 t·ha^{-1}·a^{-1}. The average TN load from soil erosion at Datong Station over the 1901–2010 period was 1.77 million tonnes. The minimum and maximum values of TN load from soil erosion were 0.001 t·ha^{-1}·a^{-1} in 1901 and 0.016 t·ha^{-1}·a^{-1} in 1964, respectively. As shown in Fig. 3, higher values of TN load from soil erosion were mainly distributed at S1, S2 and S7 sub basins.

Six classes of TN load from soil erosion in the Yangtze River Basin could be identified: 0.00–0.01, 0.01–0.05, 0.05–0.10, 0.10–0.20, 0.20–0.50 and >0.50 t·ha^{-1}·a^{-1}. Regarding the average annual TN load from soil erosion in the Yangtze River Basin over the 1901–2010 period, the classes of 0–0.01, 0.01–0.05, 0.05–0.10, 0.10–0.20, 0.20–0.50 and >0.50 t·ha^{-1}·a^{-1} accounted for total areas of 58.60%, 31.50%, 6.27%, 2.93%, 0.70%, 0.00% respectively (Table 5). 0.01 and 0.03% of the total areas of the S2 and S7 sub-basins, respectively, were characterised by TN load from soil erosion >0.50 t·ha^{-1}·a^{-1}.

The average annual TP load from soil erosion in the Yangtze River Basin over the 1901–2010 period was 0.0033 t·ha^{-1}·a^{-1}. The average annual total TP load from soil erosion at Datong Station over the 1901–2010 period was 0.56 million tonnes. The minimum and maximum values of TP load from soil erosion were 0.0004 t·ha^{-1}·a^{-1} in 1901 and 0.0051 t·ha^{-1}·a^{-1} in 1964, respectively. As shown in Fig. 4, higher values of TP load from soil erosion were mainly concentrated in the S1, S2 and S7 sub-basins.

Six classes of TP load from soil erosion in the Yangtze River Basin could be identified: 0.000–0.001, 0.001–0.005, 0.005–0.020, 0.020–0.050, 0.050–0.100 and >0.100 t·ha^{-1}·a^{-1}. Regarding the average annual TP load in the Yangtze River Basin over the 1901–2010 period, the classes of 0.000–0.001, 0.001–0.005, 0.005–0.020, 0.020–0.050, 0.050–0.100 and > 0.100 t·ha^{-1}·a^{-1} accounted for total areas of 38.11, 37.15, 18.71, 5.32, 0.71, 0.00%, respectively (Table 6). 0.22, 0.04, 0.02 and 0.01% of the total areas of the S1, S7, S8 and S2 sub-basins where characterised by TP load from soil erosion >0.1 t·ha^{-1}·a^{-1}.

3.2.1. *Spatial autocorrelation (Moran'sI)*

Moran'sIvalues of average annual soil erosion, and TN and TP loads from soil erosion were 0.39, 0.35 and 0.37, respectively. These three

Table 4
Area proportion of the mean average annual soil erosion during 1901–2010.

Class (t·ha^{-1}·a^{-1})	YRB (%)	S1 (%)	S2 (%)	S3 (%)	S4 (%)	S5 (%)	S6 (%)	S7 (%)	S8 (%)	S9 (%)	S10 (%)	S11 (%)	S12 (%)
0–5	39	29	13	48	59	63	85	24	39	52	35	51	52
5–25	38	40	36	41	34	30	12	36	43	39	50	39	39
25–50	11	13	21	7	5	4	2	15	9	5	11	7	6
50–80	5	6	13	2	2	1	1	7	4	2	3	2	2
80–150	4	6	11	1	1	1	1	8	3	1	1	1	1
>150	3	5	7	0	0	0	0	10	1	0	0	0	0

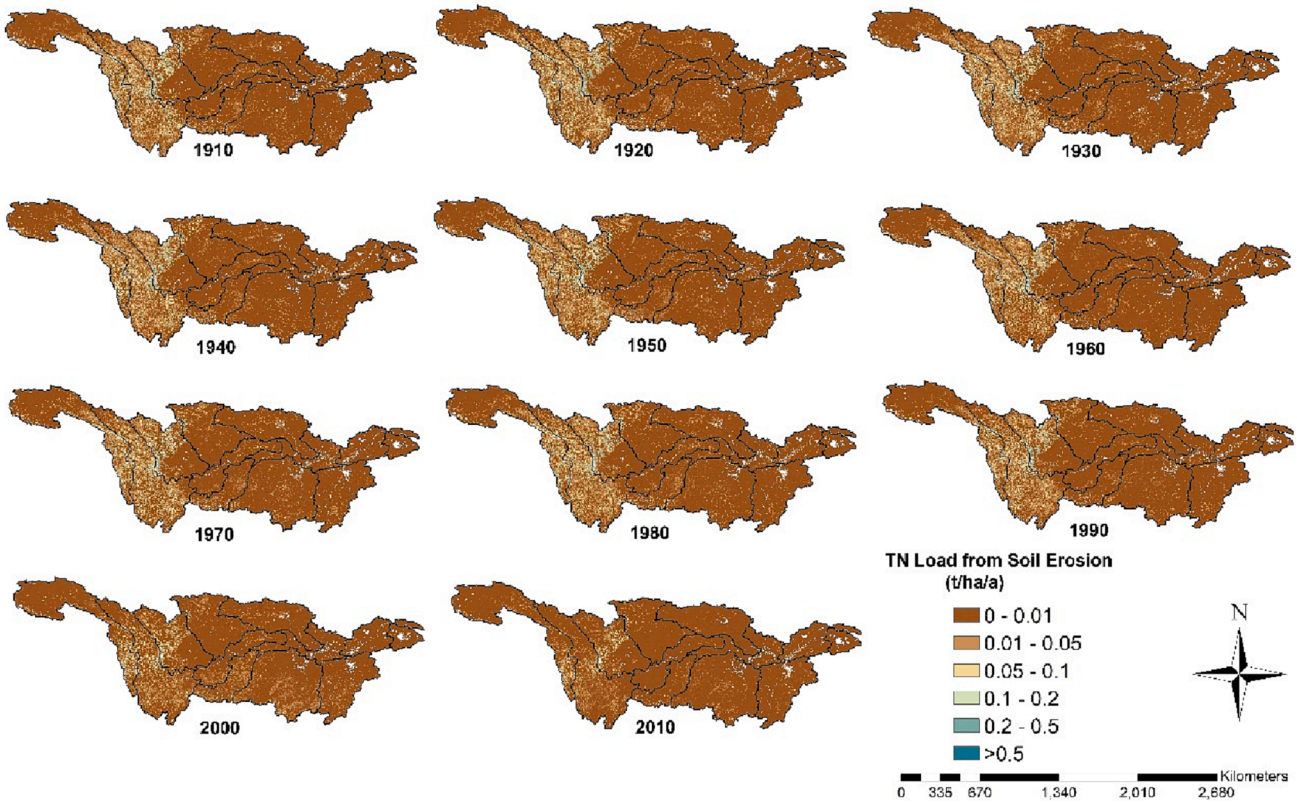

Fig. 3. Spatial and temporal variations of the TN load from natural soil erosion in the Yangtze River Basin over the 1910–2010 period.

Table 5
Area proportion of the average annual TN load from soil erosion during 1901–2010.

Class ($t \cdot ha^{-1} \cdot a^{-1}$)	YRB (%)	S1 (%)	S2 (%)	S3 (%)	S4 (%)	S5 (%)	S6 (%)	S7 (%)	S8 (%)	S9 (%)	S10 (%)	S11 (%)	S12 (%)
0.00–0.01	59	47	36	90	91	95	98	31	75	90	79	88	93
0.01–0.05	32	39	47	10	9	5	2	43	21	9	20	12	7
0.05–0.10	6	9	11	0	0	0	0	13	3	0	1	1	0
0.10–0.20	3	4	4	0	0	0	0	8	1	0	0	0	0
0.20–0.50	1	1	1	0	0	0	0	4	1	0	0	0	0
>0.50	0	0	0	0	0	0	0	0	0	0	0	0	0

auto-correlation values illustrate that the spatial distribution patterns of natural soil erosion, and TN and TP loads from soil erosion were clustering rather than random. Spatial autocorrelations of soil erosion, and TN and TP loads from soil erosion were not significant in most sub-basins. Sub-basins involving significant results mainly exhibited H-H and L-L aggregation. As revealed by the local spatial correlation pattern in the LISA cluster maps (Fig. 5), L-L areas were mainly distributed in S1, S3, S4, S5, S6, S7, S8, S9, S10, S11 and S12 and H-H areas were chiefly distributed in S1, S2 and S7.

H-H areas were mainly distributed in the southern and western areas of the Yangtze River Basin, where the altitude is relatively higher. L-L areas were primarily located in the S1, S3, S4, S5, S6, S7, S8, S9, S10, S11 and S12 sub-basins. The LISA cluster map of the average annual TN load from soil erosion shows that the L-L and H-H areas accounted for 9.0 and 38.6% of the total area, respectively. The LISA cluster map of the average annual TP load from soil erosion shows that the L-L and H-H areas accounted for 8.9 and 35.9% of the total area, respectively. The LISA cluster map of the average annual soil erosion shows that the L-L and H-H areas accounted for 25.7 and 9.9% of the total area, respectively.

3.3. Temporal variation

The average annual sediment load simulated by NLEM over the 1901–2010 period at Datong Station, representing the watershed control area of 1.7054 million km^2 of the Yangtze River Basin, was 432 million tonnes, with the maximum and minimum values of sediment load were 664 million tonnes in 1964 and 55 million tonnes in 1901. The average annual TN load from soil erosion in the watershed control area was 1.8 million tonnes, with the maximum and minimum values being 2.7 million tonnes in 1964 and 0.2 million tonnes in 1901, respectively. The average annual TP load from soil erosion in the watershed control area was 0.6 million tonnes, with the maximum and minimum values being 0.9 million tonnes in 1964 and 0.06 million tonnes in 1901, respectively.

3.3.1. Sequential T-test analysis of regime shift (STARS)

As shown in Fig. 7, regime shift of soil erosion occurred in 2004, with the regime shift index (RSI) being −1.24. The regime shifts of the sediment load at Datong Station and those of the TN and TP loads from soil erosion occurred at similar times. Regime shifts of the TN load from soil erosion occurred in 1969 (RSI = -0.53), 1986 (RSI = -0.72), 2000 (RSI = -1.57) and 2006 (RSI = -0.12). In terms of AP, regime shifts of the TP load from soil erosion occurred in 1969 (RSI = -0.54), 1986 (RSI =

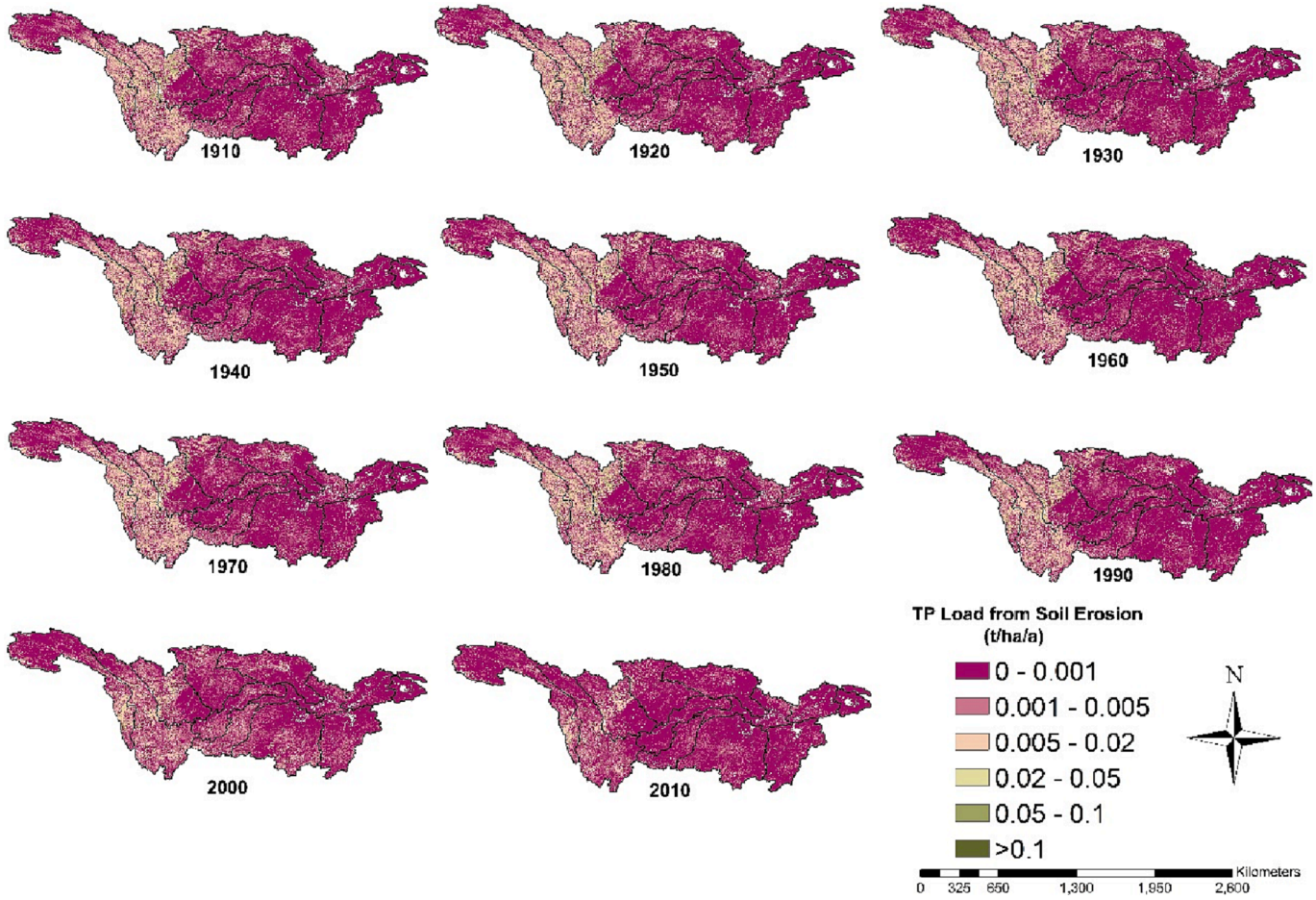

Fig. 4. Spatial and temporal variations of the TP load from soil erosion in the Yangtze River Basin over the 1910–2010 period.

Table 6
Area proportion of the average area of mean annual TP load from soil erosion during 1901–2010.

Class ($t \cdot ha^{-1} \cdot a^{-1}$)	YRB (%)	S1 (%)	S2 (%)	S3 (%)	S4 (%)	S5 (%)	S6 (%)	S7 (%)	S8 (%)	S9 (%)	S10 (%)	S11 (%)	S12 (%)
0.000–0.001	38	29	15	57	55	75	80	20	43	50	51	64	67
0.001–0.005	37	37	38	37	38	22	17	34	40	41	40	31	30
0.005–0.020	19	24	36	6	7	3	3	27	13	9	9	5	3
0.020–0.050	5	8	10	0	0	0	0	13	3	1	0	0	0
0.050–0.100	1	1	1	0	0	0	0	5	1	0	0	0	0
>0.100	0	0	0	0	0	0	0	0	0	0	0	0	0

-0.70), 1999 (RSI = -1.23) and 2006 (RSI = -0.58). Regime shifts of the sediment load at Datong Station occurred in 1969 (RSI = -0.52), 1985 (RSI = -0.64) and 2001 (RSI = -1.84).

3.3.2. *Mann–Kendall trend tests*

Fig. 8 presents the results of the M−K trend tests of soil erosion in the Yangtze River Basin, sediment load at Datong Station, and TN load and TP loads from soil erosion. The soil erosion trend in the Yangtze River Basin is not significant because the UF line is within the 95% confidence level. The jump time (intersect point of UF and UB lines) is around in 2001 (within at 95% confidence level), meaning that, over the entire 1901–2010 period, 2001 was a soil erosion changing point. The STARS method also indicated a regime shift in 2001. The annual precipitation in the Yangtze River Basin in 2002 was 1439.08 mm, i.e., relatively increased compared to values over the entire 1901–2010 period.

An increasing soil erosion trend occurred from 1901 to 1929, as shown in Fig. 8. Subsequently, from 1932 to 1951, soil erosion decreased and began to oscillate during the 1952–1973. From 1973 to 1993, soil erosion declined and subsequently increased from 1993 to 2005. From 2005 up until 2010, it followed a descending trend.

The sediment load at Datong Station, and TN load and TP loads from soil erosion exhibited similar variations, all of them started exhibiting decreasing trends in 1968, which became significant in 1978 (within the 95% confidence level). M−K trend tests indicated that the intersection of the UF and UB lines (jump time) of sediment load of Datong Station and TN and TP loads from soil erosion was around 1990 (within the 95% confidence level), thereby being suggestive of a changing point in 1990. Nevertheless, the STARS method did not indicate a changing point in 1990.

As shown in Fig. 8, the sediment load at Datong Station and the TN and TP loads from soil erosion followed increasing trends from 1901 to 1930. During the 1932–2010 period, the sediment load at Datong Station and TP load from soil erosion followed overall decreasing trends. The TN load from soil erosion also decreased from 1932 to 1950, while it followed an increasing trend from 1950 to 1960 and from 1965 to 1972. The TN load from soil erosion continued to decrease after 1972.

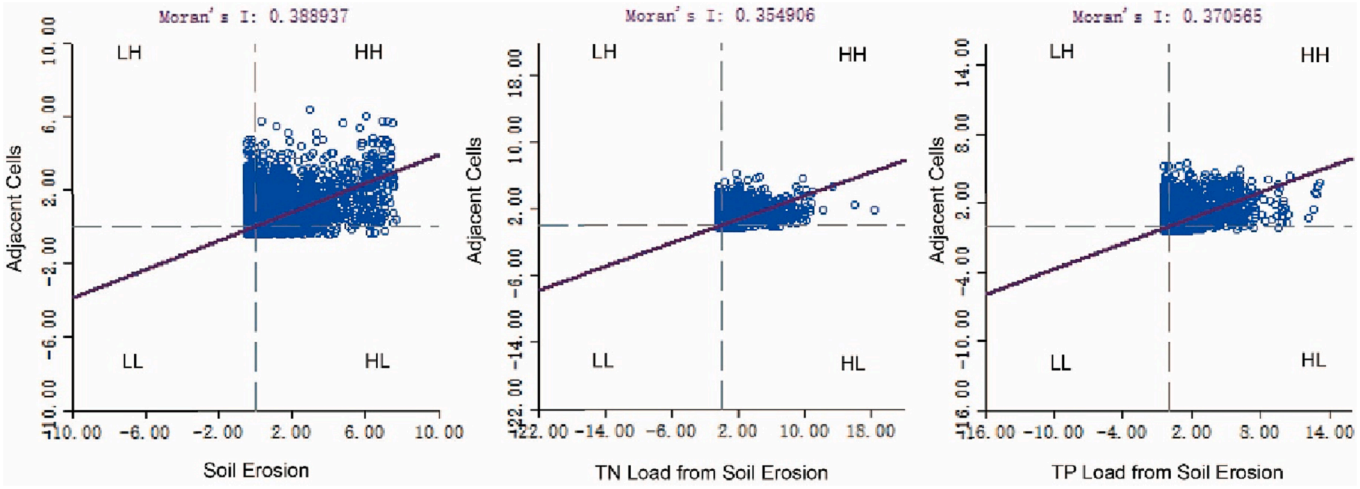

Fig. 5. Moran'sIscatter plots of the average annual soil erosion, and TN and TP loads from soil erosion in the Yangtze River Basin. The first, second, third and fourth quadrants of the coordinate system are H-H, L-H, L-L and H-L areas, respectively.

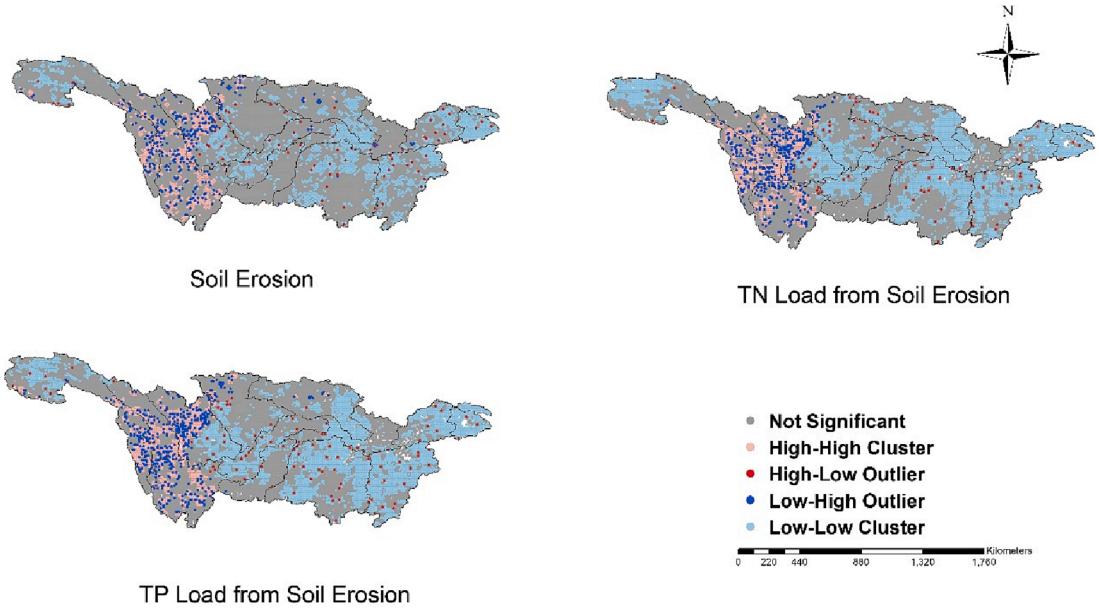

Fig. 6. Spatial autocorrelation image of average annual soil erosion, and TN and TP loads from soil erosion over the 1901–2010 period.

3.3.3. Wavelet analysis

In environment sciences, wavelet analysis could be applied to analyse multi-scale, irregular, unstable and noisy time series (Cazelles et al., 2008). The principle periodic component and transient dynamics in a given time series could be interpretated by the wavelet power spectrum. Regarding soil erosion in the Yangtze River Basin, there was higher variance between 0.0 and 1.2 years in 1915, 1950, 1970 and 1995 (Fig. 9), greater wavelet power was evident between 2.4 and 3.2 years around 1937–1943, An area of significant variance with periods between 3.8 and 5.7 years was evident between 1995 and 2003, an area of significant variance with periods between 15.8 and 25.6 years was also evident between 1990 and 2010. On this account, high wavelet power existed over long periods of time. The global wavelet spectrum implied peaks at 1.4, 4, 15.8 and 35.2 years.

Regarding sediment load of Datong Station, there was a band of higher variance between 0.0 and 6.0 years around 1901–1905 (significant at the 95% confidence level), between 0.8 and 2.4 years, greater wavelet power with significant variance was evident around 1956 and 1995. From 1962 to 1972, periods are between 0.0 and 3.3 years with significant confidence level at the 95%. The global wavelet spectrum implied peaks at 0.8, 2.4, 5.6, 8, 16 and 35.2 years. Between 7.2 and 8 years, between 8.0 and 9.6 years and between 12.8 and 19.2 years, greater wavelet power appeared during 1975–1987, 1958–1970 and 1995–2010 which were not significant at 95% confidence level.

For the TN and TP loads from soil erosion, wavelet power spectrum and global wavelet spectrum were quite similar. The global wavelet spectrum of TN and TP loads from soil erosion in the Yangtze River Basin illustrated peaks at 1.0, 2.7, 5.6, 8, 16.0 and 35.2 years. During 1901–1905, a contour appeared between 0.0 and 6.0 years (significant at the 95% confidence level). Between 0.5 and 1.6 years, there was a high power from 1994 to 1996. Moreover, it was significant at 95% confidence level. There was a high variance between 0 and 3.2 years with 5% significance regions of power from 1964 to 1972. Between 0.8 and 3.2 years, 95% significant confidence level contour existed from 1957 to 1960. This was a little bit different from the spectrum of the sediment load at Datong Station. There were also two greater, albeit not significant at the 95% confidence level, power intervals from 1957 to 1969, and from 1998 to 2010 between 8.0 and 9.6 years and between

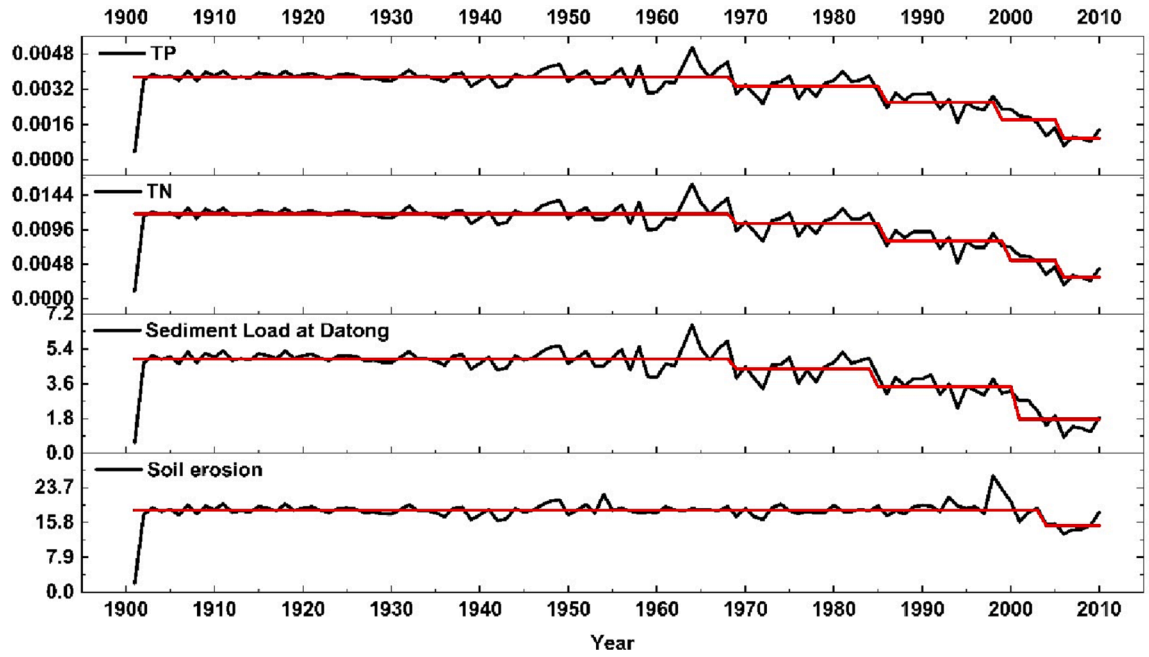

Fig. 7. Detection of regime shift of soil erosion and sediment load at Datong Station, as well as TN and TP loads from soil erosion. Black lines represent the initial data of the indicators. Red lines indicate the equal-weighed arithmetic means of the regimes. The units of the TP and TN loads sediment load and soil erosion are $t{\cdot}ha^{-1}{\cdot}a^{-1}$, $t{\cdot}ha^{-1}{\cdot}a^{-1}$, 100 million tonnes, $t{\cdot}ha^{-1}{\cdot}a^{-1}$, respectively.

14.4 and 17.6 years, respectively.

4. Discussion

It has been verified that human activities, such as, dam operations, deforestation, have impact on the sediment loads in basin (Zhang et al., 2006). There were 11,931 water reservoirs which were mainly located in the tributaries had been constructed by the end of 1980s (Zhang et al., 2006). These reservoirs would trap sediments and reducing downstream sediment loads. The condition are more complicated in the mainstream of Yangtze River Basin compared with tributaries. Precipitation, transport process, water discharge, Dam operations, large lakes, changing slope of river bed and changing patterns would have influences on the sediment loads in stations of mainstream (Zhang et al., 2006).

In general, higher soil erosion values were mainly distributed in the S1, S2 and S7 sub-basins of the Yangtze River Basin. The S1, S2 and S7 sub-basins are situated at higher elevations, comprising mountainous and hilly regions in the Yangtze River Basin, hence, in general, more severe soil erosion conditions could be experienced (Alewell et al., 2008). This highlights the need for more thorough investigations in the upper reaches.

The types of land cover in the upper reaches are mainly plateau grassland and bare land, this is the primary cause of the widely distributed soil loss in the upper reaches (Li et al., 2022). The deterioration of water quality in upstream of Yangtze River hindered the development of the YRB (Li et al., 2009). It has also been validated that the primary non-point pollution sources of upper reaches is soil erosion (Wu et al., 2012). It has been validated by the watershed of Fuji River and Yellow River that natural areas was the major sources of AN and AP pollutions (Tao et al., 2010). Nutrient balance of Lancang River was also influenced by cascade dam construction. In Lancang River, rainfall was the main factor of soil erosion which accounted for 60% TP load (Zhang et al., 2020a).

Higher values of TN load from soil erosion were mainly distributed at the S1, S2 and S7 sub-basins, which might because the TN content in soil erosion were relatively high compared with other sub-basins. These upstream of YRB contributed considerable TN loss from soil (Chen et al., 2018; Wang et al., 2015b; Wang et al., 2019b). DN loss spatial distribution was different from AN loss spatial distribution, as middle and lower reaches are the primary areas of TN load (Wang et al., 2020). Higher TP content of soil was mainly distributed in S1, S2 and S7 and this might contribute to the higher values of TP load from soil erosion. It has been discussed that the lower AN and AP from headwater of YRB might because the lower precipitation and the land use type was grassland which have effective ability of soil retention (Tao et al., 2010). It has been demonstrated that the DN and DP spatial distribution were quite different from AN and AP and this indicated that management efforts should include both human activities and contributing factors management (Tao et al., 2010).

The degree of soil loss in the upper reaches of Yangtze River Basin is generally severe. In addition, human activities are low, while crop land and built-up land occupy together only about 20% of the entire land area, hence, other pollution sources do not contribute significantly to the TN and TP emissions (Alewell et al., 2020; Liu et al., 2020). It has been validated that the upstream of Yangtze River Basin contribute more to the nutrient loss compared with the middle and lower reaches (Zhang et al., 1999). In the lower reaches of the Yangtze River Basin, other sources of TN and TP, such as urban domestic sewage and non-point sources were relatively large compared with those in the upper reaches (Li et al., 2022).

The average TN/TP ratio of sediment load from soil erosion at Datong Station was 3.14 over the 1901–2010 period. Over the 1960–2003 period, the average TN/TP ratio was 6.35, while the average DN/DP ratio was 18.145 in the upstream of Yangtze River (Shen et al., 2013). Therefore, over the 1960–2003 period, the AN/AP ratio from the upper reaches of Yangtze River must have been below 6.35. In addition, dam constructions after 1968 (Yang et al., 2018), resulted in economic development and water pollution. Moreover, the DN and DP increased from 1980 because of intensive water pollution (Shen et al., 2013). The effect of water pollution on the value of TN and TP values was identifiable, since the DN and DP values in 2003 were triple of the value in 1960, hence, the TN and TP values in 1960 were relatively more reasonable. The TN/TP ratio in 1960 was 4.08, with the DN/DP ratio being 18.91, therefore, the AN/AP ratio was definitely <4.08, thereby matching nicely the result of this research. In the upper reach of the YRB, the DN/DP value ranged from 15.3 to 20.2. Before 2000, runoff in Upper

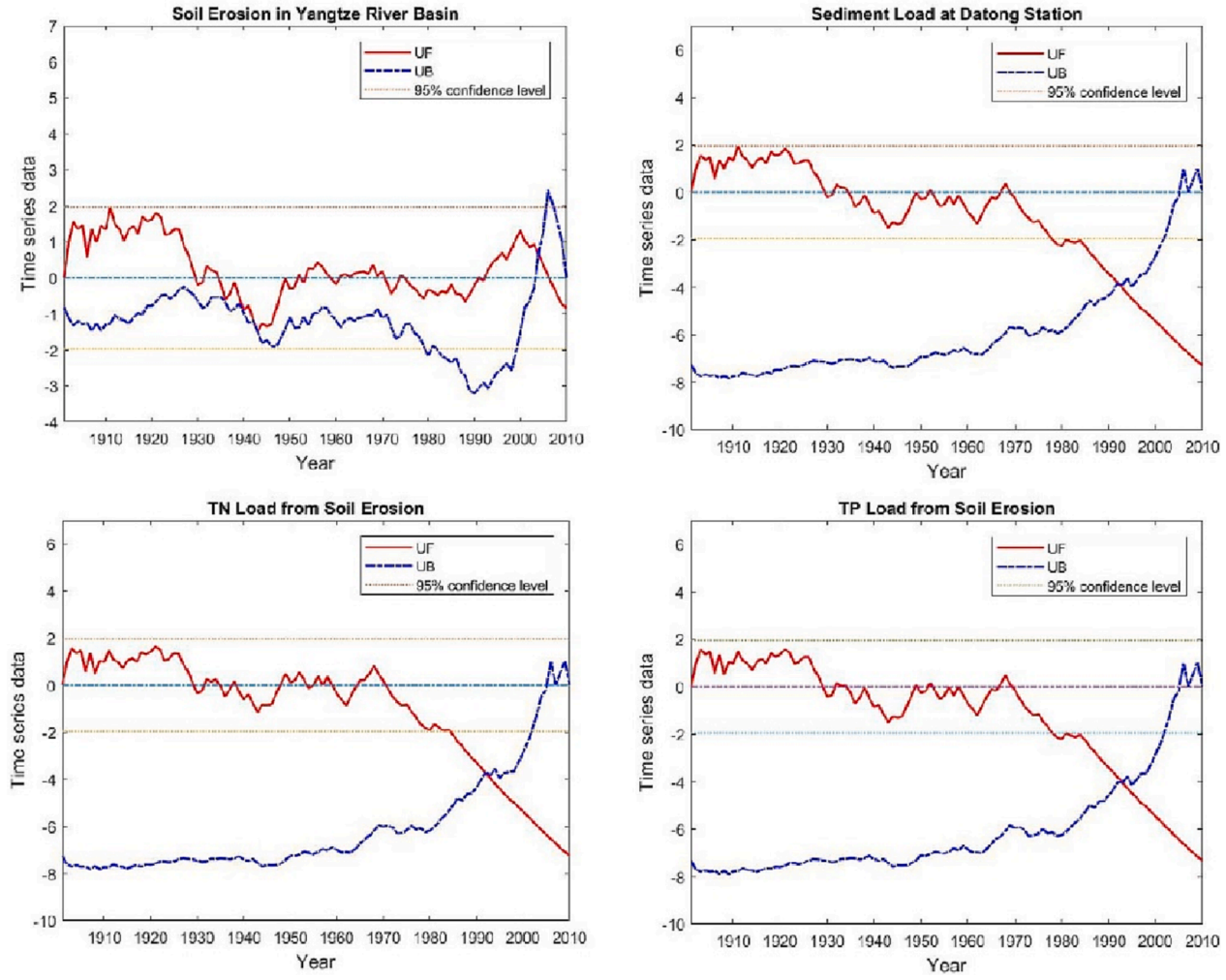

Fig. 8. Mann-Kendall trend tests of soil erosion in the Yangtze River Basin, sediment load in Datong Station, and TN and TP loads from soil erosion. Red, blue and yellow lines represent UF, UB and the 95% confidence level, respectively.

reach of YRB was N limited and after that, P became more limited. It has been expected that after the TGD operation, more AP would be deposited in the reservoir as the P is more particle reactive and this gave rise to the algal blooms (Tao et al., 2010). The average annual AN/AP ratio over the 1901–2010 period in the S1, S2, S3, S4, S5, S6, S7, S8, S9, S10, S11 and S12 sub-basins were 3.06, 3.32, 2.74, 2.28, 2.69, 2.97, 3.36, 2.40, 2.08, 3.50, 3.49 and 3.39, respectively.

The L-L areas were located in regions with high population density and intense human activities. As shown in Fig. 6, the scatter points are mainly in the first quadrants, revealing strong positive spatial correlations among soil erosion, and the TN and TP loads from soil erosion (Xiong et al., 2021).

The maximum values of TN and TP loads from soil erosion in 1964 were because the actual sediment load at Datong Station was maximum from 1901 to 2010 in Yangtze River Basin. The minimum values of sediment load at Datong Station, as well as those of the TN and TP loads from soil erosion, in 1901 were due to the annual precipitation over Yangtze River being as low as 243.34 mm. One of the primarily driving forces of soil erosion is precipitation, with more intense rainfall causing severe soil loss and exacerbating the TN and TP loads from soil erosion (B. Zhang et al., 2020). Furthermore, raster rainfall data were input in the NLEM model, consequently, the TN and TP loads from soil erosion were related with them. The maximum values indicated that regardless of rainfall being one of the driving forces of the TN and TP loads from soil erosion, there may be also other elements contributing to increases in the variabilities of the TN and TP loads from soil erosion (B. Zhang et al., 2020).

Regarding STARS method, regime shift of soil erosion occurred in 2004, and the Three Gorges Dam (TGD) trial operation occurred in 2003, this might have resulted in further land use changes in the Yangtze River Basin (Zhang et al., 2020b). 60% of sediment entered into the Three Gorges Dam and was trapped by the dam (Xu and Milliman, 2009).The regime shifts of the sediment load at Datong Station and those of the TN and TP loads from soil erosion occurred at similar times. N and P balance in YRB were influenced by the Three Gorges Dam operation and TN and DIN and TP loads decreased after 2003 (Sun et al., 2013). Gezhouba Dam operated during 1981–1986 and may have been the cause for the regime shift of AN, AP and sediment load at Datong Station occurred around 1985 (Zhang et al., 2006). The regime shift of the sediment load at Datong Station, as well as those of the TN and TP loads from soil erosion, in 1969 might have been the result of sediment retention by dams, whose impact on Yangtze River Basin in 1968 (Fang et al., 2019).

M−K trend tests indicated that a changing point of sediment load of Datong Station and TN and TP loads from soil erosion was in 1990. This may have been connected with Gezhouba Dam, which operated during 1981–1986 (Zhang et al., 2006). The operation of Gezhouba Dam could have reduced the mainstream sediment of the Yangtze River Basin, with a certain amount of sediment ending up in Poyang lake (Zhang et al., 2006).

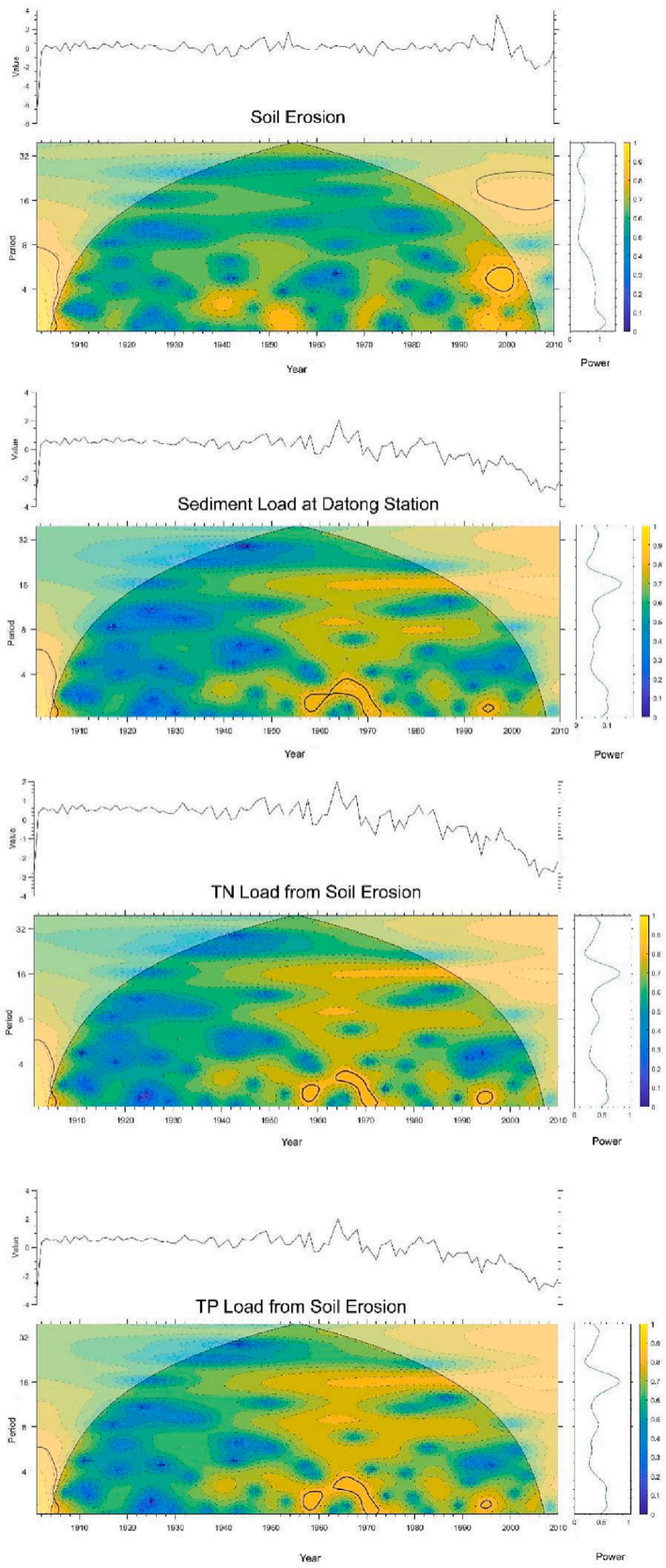

Fig. 9. Wavelet power spectrum of soil erosion, sediment load at Datong Station, and TN and TP loads from soil erosion. In each panel, the upper part illustrates the standardised time series of the indicator; the lower right panel displays the global wavelet spectrum; the lower left panel displays the wavelet power spectrum (Morlet) plotted by power $\log_2$ form. Thick black contours in the wavelet power spectrum indicate the 95% confidence level against red noise. Cone of influence (COI), which delimits the region not influenced by edge effects is expressed by semi-circular black curves. In the wavelet power spectrum, dashed black contours illustrate z level.

It has been demonstrated that total sand mined in mainstream (the middle and lower reaches) of Yangtze River Basin increased from 23 MT in 2004 to 60 MT in 2010 (Chen et al., 2020). This might be another reason for sediment decrease at Datong Station. Sand and sediments are essential materials for habitats. The decrease of sediment and loss of sand gave rise to the degradation of aquatic habitats particularly in downstream of Dam (Chen et al., 2017). As the soil erosion condition in the upper reach of YRB was severe, control erosion by maintaining vegetation in these areas are necessary (Chen et al., 2017). The changing pattern at Datong Station was similar with Hankou Station. However, as Poyang Lake adopted quite amounts of sediments and river channel had effect on sediments, the decreasing trend stronger than Hankou (Zhang et al., 2006). Actually, there are poor correlation of these two stations between sediments and runoff, this was because the impact of reservoir on sediment loads was so tremendous to overwhelm the regular of more water discharge would have more power to transport sediments (Zhang et al., 2006). It has also demonstrated that Dongting Lake had more influences on the decrease at Datong Station compared with Poyang Lake (Zhang et al., 2006).

There was a lack of scientific monitored and estimation of absorbed nitrogen and phosphorus carried by sediment on account of the standard of China surface water quality (GB3838-2002) of water sampling. This research could make up for the lack of data for the Yangtze River Basin from 1901 to 2010. As the sediment load data applied for SDR calculation and soil erosion and TN and TP load from soil erosion estimation was only from Datong Station which could represent the whole basin of the Yangtze River Basin, the SDR value for the 12 sub-basins were same. If the hydrologic control station of 12 sub-basins could be available in the future, the sediments load, and TN and TP loads from soil erosion contributed to the whole basin could be more accurate and interpretable.

5. Conclusion

Nitrogen and phosphorus are essential elements for organism living, however, on account of the measured data is insufficient, the estimation data of these parameters are restricted. This study calculated the soil erosion, and total nitrogen (TN) and total phosphorus (TP) loads from soil erosion in the Yangtze River Basin based on the Revised Universal Soil Loss Equation (RUSLE) model and Nutrient Losses Empirical Model (NLEM) methods using precipitation, digital elevation models (DEM), soil erodibility factor, normalized difference vegetation index (NDVI), land use type from remote sensing data, soil properties data, and analysed the spatio-temporal distributions characteristics of soil erosion, and TN and TP loads from soil erosion. The main conclusions are as follows:

In 2000, the relative error was −3.14% and in 2004, the relative error was −14.07%, indicating that the model was reasonable. The calculated average sediment delivery ratio (SDR) background in the Yangtze River Basin based on this method was 0.1557. This SDR value which was get rid of the impact of dam trap was applied for the calculation of sediment loads in the Datong station. Over the 1901–2010 period, the average annual soil erosion in the Yangtze River Basin was 18.38 $t{\cdot}ha^{-1}{\cdot}a^{-1}$. Soil erosion in the S1, S2 and S7 sub-basins was higher compared with other sub-basins of Yangtze River Basin, this was due to land cover at the upper reaches of the Yangtze River Basin being mainly plateau grassland and bare land. This highlights the need for more thorough investigations in the upper reaches. Over the 1901–2010 period, the average annual TN and TP loads from soil erosion in the Yangtze River Basin were 0.0100 and 0.0033 $t{\cdot}ha^{-1}{\cdot}a^{-1}$, respectively, the average values of TN and TP loads from soil erosion at Datong Station from 1901 to 2010 were 1.77 and 0.56 million tonnes, respectively. The average TN/TP value of sediment load at Datong Station from soil erosion was 3.14.

The Moran's Index of the average annual soil erosion, and TN and TP loads from soil erosion indicate that the soil erosion, and TN and TP loads from soil erosion were positively related, with the spatial distribution patterns being clustering rather than random. High-High cluster areas were mainly evident in the high-altitude regions in the western and southern Yangtze River Basin. Low-Low cluster areas were scattered primarily in regions of high population density and intense human activities. According to NLEM, over the 1901–2010 period, the average annual sediment load at Datong Station, representing the watershed control area of 1.7054 million km^2 of the Yangtze River Basin was 432 million tonnes, while the average total TN and TP loads from soil erosion at Datong Station were 1.77 and 0.56 million tonnes, respectively.

There was a jump time around 2001 of soil erosion, which means that, over the entire 1901–2010 period, 2001 was a changing point in soil erosion. Mann-Kendall (M−K) trend tests indicated that the jump points of sediment load of Datong Station, and TN load and TP loads from soil erosion occurred around 1990, hence, 1990 may have been also a changing point, likely due to the operation of Gezhouba Dam during 1981–1986. Regarding soil erosion in the Yangtze River Basin, there was higher variance between 0.0 and 1.2 years in 1915, 1950, 1970 and 1995. The global wavelet spectrum of the TN and TP loads from soil erosion in the Yangtze River Basin indicated peaks at 1.0, 2.7, 5.6, 8.0, 16.0 and 35.2 years.

In the process of SDR calculation, soil erosion and AN and AP estimation was only from Datong Station which could represent the whole basin of the Yangtze River Basin. The shortcoming of this research is the SDR value for the 12 sub-basins were same. As the representative hydrologic control station of 12 sub-basins become available in the future, the spatial variation of sediments load, and AN and AP contributed to the whole basin could be more accurate and interpretable. TN and TP at Datong Station could be estimated when the dissolved nitrogen and phosphorus are modeled in future depth research.

CRediT authorship contribution statement

Xixi Liu: Conceptualization, Methodology, Data curation, Formal analysis, Investigation, Validation, Visualization, Writing – original draft, Writing – review & editing. **Yufei Bao:** Conceptualization, Investigation, Writing – review & editing. **Yuchun Wang:** Conceptualization, Supervision, Methodology, Writing – review & editing. **Di Zhang:** Investigation, Resources, Data curation. **Mingming Hu:** Conceptualization, Formal analysis. **Xinghua Wu:** Investigation, Resources, Data curation. **Jie Wen:** Investigation, Resources. **Shanze Li:** Investigation, Resources. **Meng Sun:** Investigation, Resources.

Declaration of Competing Interest

The authors declare that they have no known competing financial interests or personal relationships that could have appeared to influence the work reported in this paper.

Data availability

Data will be made available on request.

Acknowledgements

This study was supported by grants from the National Key Research and Development Program of China (2021YFC3201002); National Natural Science Foundation of China (92047204, U2040211); Key Research and Development Program of Yunnan (202203AA080009); the National Science Foundation for Young Scientists of China (Grant No. 42107283); the Project of China Three Gorges Corporation (No. 202003173). The data set is provided by National Tibetan Plateau Data Center (http://data.tpdc.ac.cn), National Earth System Science Data Center, National Science & Technology Infrastructure of China. (http://www.geodata.cn) and Resource and Environment Science and Data Center (https://www.resdc.cn/).

References

Alewell, C., Meusburger, K., Brodbeck, M., Bänninger, D., 2008. Methods to describe and predict soil erosion in mountain regions. Landsc. Urban Plan. 88 (2-4), 46–53.

Alewell, C., Ringeval, B., Ballabio, C., Robinson, D.A., Panagos, P., Borrelli, P., 2020. Global phosphorus shortage will be aggravated by soil erosion. Nat. Commun. 11 https://doi.org/10.1038/s41467-020-18326-7.

Alexander, R.B., Böhlke, J.K., Boyer, E.W., David, M.B., Harvey, J.W., Mulholland, P.J., Seitzinger, S.P., Tobias, C.R., Tonitto, C., Wollheim, W.M., 2009. Dynamic modeling of nitrogen losses in river networks unravels the coupled effects of hydrological and biogeochemical processes. Biogeochemistry 93 (1-2), 91–116.

Anselin, L., 1995. Local indicators of spatial association—LISA. Geogr. Anal. 27 (2), 93–115.

Beskow, S., Mello, C.R., Norton, L.D., Curi, N., Viola, M.R., Avanzi, J.C., 2009. Soil erosion prediction in the Grande River Basin, Brazil using distributed modeling. Catena (Amst) 79 (1), 49–59.

Chen, D., Shen, H., Hu, M., Wang, J., Zhang, Y., Dahlgren, R.A., 2018. Legacy Nutrient Dynamics at the Watershed Scale: Principles, Modeling, and Implications, in: Advances in Agronomy. https://doi.org/10.1016/bs.agron.2018.01.005.

Chen, Y., Zhang, S., Huang, D., Li, B.-L., Liu, J., Liu, W., Ma, J., Wang, F., Wang, Y., Wu, S., Wu, Y., Yan, J., Guo, C., Xin, W., Wang, H., 2017. The development of China's Yangtze River Economic Belt: how to make it in a green way? Sci. Bull. (Beijing) 62 (9), 648–651.

Chen, Y., Qu, X., Xiong, F., Lu, Y., Wang, L., Hughes, R.M., 2020. Challenges to saving China's freshwater biodiversity: Fishery exploitation and landscape pressures. Ambio 49 (4), 926–938.

Chuenchum, P., Xu, M., Tang, W., 2020. Predicted trends of soil erosion and sediment yield from future land use and climate change scenarios in the Lancang-Mekong River by using the modified RUSLE model. Int. Soil Water Conservat. Res. 8 (3), 213–227.

Cilek, A., Berberoglu, S., Kirkby, M., Irvine, B., Donmez, C., Erdogan, M.A., 2015. Erosion modelling in a Mediterranean Subcatchment under climate change scenarios using Pan-European Soil Erosion Risk Assessment (PESERA), in: International Archives of the Photogrammetry, Remote Sensing and Spatial Information Sciences - ISPRS Archives. https://doi.org/10.5194/isprsarchives-XL-7-W3-359-2015.

Dabral, P.P., Baithuri, N., Pandey, A., 2008. Soil erosion assessment in a hilly catchment of North Eastern India using USLE, GIS and remote sensing. Water Resour. Manage. 22. https://doi.org/10.1007/s11269-008-9253-9.

Ding, X.W., Hou, B.D., Xue, Y., Jiang, G.H., 2017. Long-term effects of ecological factors on nonpoint source pollution in the upper reach of the Yangtze river. J. Environ. Inf. https://doi.org/10.3808/jei.201700370.

Ding, Y., Peng, S., 2020. Spatiotemporal trends and attribution of drought across China from 1901–2100. Sustainability (Switzerland) 12 (2), 477.

Ding, X., Shen, Z., Hong, Q., Yang, Z., Wu, X., Liu, R., 2010. Development and test of the Export Coefficient Model in the Upper Reach of the Yangtze River. J. Hydrol. (Amst) 383 (3-4), 233–244.

Ding, X.W., Shen, Z.Y., Liu, R.M., Chen, L., Lin, M., 2014. Effects of ecological factors and human activities on nonpoint source pollution. Hydrol. Earth Syst. Sci. Discuss 11, 691–721. https://doi.org/10.5194/hessd-11-691-2014.

Dong, L., Lin, L., Tang, X., Huang, Z., Zhao, L., Wu, M., Li, R., 2020. Distribution characteristics and spatial differences of phosphorus in the main stream of the Urban River stretches of the middle and lower reaches of the Yangtze River. Water (Switzerland) 12 (3), 910.

Duan, S., Liang, T., Zhang, S., Wang, L., Zhang, X., Chen, X., 2008. Seasonal changes in nitrogen and phosphorus transport in the lower Changjiang River before the construction of the Three Gorges Dam. Estuar. Coast Shelf Sci. 79 (2), 239–250.

Duan, Y.u., Xu, G., Liu, Y., Liu, Y., Zhao, S., Fan, X., 2020. Tendency of runoff and sediment variety and multiple time scalewavelet analysis in Hongze Lake during 1975–2015. Water (Switzerland) 12 (4), 999.

Fan, G.Y., Cowley, J.M., 1985. Auto-correlation analysis of high resolution electron micrographs of near-amorphous thin films. Ultramicroscopy 17 (4), 345–355.

Fang, G., Yuan, T., Zhang, Y., Wen, X., Lin, R., 2019. Integrated study on soil erosion using RUSLE and GIS in Yangtze River Basin of Jiangsu Province (China). Arab. J. Geosci. 12 https://doi.org/10.1007/s12517-019-4331-2.

Ganasri, B.P., Ramesh, H., 2016. Assessment of soil erosion by RUSLE model using remote sensing and GIS – a case study of Nethravathi Basin. Geosci. Front. 7 (6), 953–961.

Griffith, D.A., 1987. Spatial autocorrelation: a primer. Spatial autocorrelation: a primer. https://doi.org/10.2307/143927.

Guo, L., Li, Z., 2003. Effects of nitrogen and phosphorus from fish cage-culture on the communities of a shallow lake in middle Yangtze River basin of China. Aquaculture 226 (1-4), 201–212.

Jain, S.K., Kumar, S., Varghese, J., 2001. Estimation of soil erosion for a Himalayan watershed using GIS technique. Water Resour. Manag. 15 https://doi.org/10.1023/A:1012246029263.

Jing, Y., Zhang, F., He, Y., Kung, H.-t., Johnson, V.C., Arikena, M., 2020. Assessment of spatial and temporal variation of ecological environment quality in Ebinur Lake Wetland National Nature Reserve, Xinjiang, China. Ecol. Indic. 110, 105874.

Kinnell, P.I.A., 2017. A comparison of the abilities of the USLE-M, RUSLE2 and WEPP to model event erosion from bare fallow areas. Sci. Total Environ. 596-597, 32–42.

Lanza, G.R., 2011. Accelerated eutrophication in the mekong river watershed: Hydropower development, climate change, and waterborne disease, in: Eutrophication: Causes, Consequences and Control. https://doi.org/10.1007/978-90-481-9625-8-19.

Li, J., Chen, Y., Cai, K., Fu, J., Ting, T., Chen, Y., Folberth, C., Liu, Y., 2022. A high-resolution nutrient emission inventory for hotspot identification in the Yangtze River Basin. J. Environ. Manage 321, 115847.

Li, S., Gu, S., Tan, X., Zhang, Q., 2009. Water quality in the upper Han River basin, China: The impacts of land use/land cover in riparian buffer zone. J. Hazard. Mater. 165 (1-3), 317–324.

Li, M., Hinnov, L., Kump, L., 2019. Acycle: Time-series analysis software for paleoclimate research and education. Comput. Geosci. 127, 12–22. https://doi.org/10.1016/j.cageo.2019.02.011.

Liu, B., Xie, Y., Li, Z., Liang, Y., Zhang, W., Fu, S., Yin, S., Wei, X., Zhang, K., Wang, Z., Liu, Y., Zhao, Y., Guo, Q., 2020. The assessment of soil loss by water erosion in China. Int. Soil Water Conserv. Res. 8 (4), 430–439.

Mirzaee, S., Ghorbani-Dashtaki, S., Mohammadi, J., Asadzadeh, F., Kerry, R., 2017. Modeling WEPP erodibility parameters in calcareous soils in northwest Iran. Ecol. Indic. 74, 302–310.

Peng, S., 2020. 1-km Monthly Precipitation Dataset for China (1901–2021). National Tibetan Plateau Data Center, 10.5281/zenodo.3185722.

Peng, S., Ding, Y., Liu, W., Li, Z., 2019. 1 km monthly temperature and precipitation dataset for China from 1901 to 2017. Earth Syst. Sci. Data 11. https://doi.org/10.5194/essd-11-1931-2019.

Penghao, C., Pingkuo, L., Hua, P., 2019. Prospects of hydropower industry in the Yangtze River Basin: China's green energy choice. Renew. Energy 131, 1168–1185.

Qu, S., Wang, L., Lin, A., Yu, D., Yuan, M., Li, C., 2020. Distinguishing the impacts of climate change and anthropogenic factors on vegetation dynamics in the Yangtze River Basin, China. Ecol. Indic. 108, 105724.

Rodionov, S.N., 2005. A sequential method for detecting regime shifts in the mean and variance. Large-scale disturbances (regime shifts) and recovery in aquatic ecosystems: Challenges for management toward sustainability.

Shangguan, W., Dai, Y., Liu, B., Zhu, A., Duan, Q., Wu, L., Ji, D., Ye, A., Yuan, H., Zhang, Q., Chen, D., Chen, M., Chu, J., Dou, Y., Guo, J., Li, H., Li, J., Liang, L.u., Liang, X., Liu, H., Liu, S., Miao, C., Zhang, Y., 2013. A China data set of soil properties for land surface modeling. J. Adv. Model. Earth Syst. 5 (2), 212–224.

Shen, Z., Chen, L., Ding, X., Hong, Q., Liu, R., 2013. Long-term variation (1960–2003) and causal factors of non-point-source nitrogen and phosphorus in the upper reach of the Yangtze River. J. Hazard. Mater. 252–253, 45–56.

Shen, L.i., Xu, H., Guo, X., Li, M., 2011. Characteristics of Large-Scale Harmful Algal Blooms (HABs) in the Yangtze River Estuary and the Adjacent East China Sea (ECS) from 2000 to 2010. J. Environ. Prot. (Irvine, Calif) 02 (10), 1285–1294.

Sonnenborg, T.O., Christiansen, J.R., Pang, B., Bruge, A., Stisen, S., Gundersen, P., 2017. Analyzing the hydrological impact of afforestation and tree species in two catchments with contrasting soil properties using the spatially distributed model MIKE SHE SWET. Agric. For. Meteorol. 239, 118–133.

Strokal, M., Kahil, T., Wada, Y., Albiac, J., Bai, Z., Ermolieva, T., Langan, S., Ma, L., Oenema, O., Wagner, F., Zhu, X., Kroeze, C., 2020. Cost-effective management of coastal eutrophication: a case study for the yangtze river basin. Resour. Conserv. Recycl. 154, 104635.

Sun, C., Shen, Z., Liu, R., Xiong, M., Ma, F., Zhang, O., Li, Y., Chen, L., 2013. Historical trend of nitrogen and phosphorus loads from the upper Yangtze River basin and their responses to the Three Gorges Dam. Environ. Sci. Pollut. Res. 20 (12), 8871–8880.

Tao, Y., Wei, M., Ongley, E., Li, Z., Jingsheng, C., 2010. Long-term variations and causal factors in nitrogen and phosphorus transport in the Yellow River, China. Estuar. Coast Shelf Sci. 86 (3), 345–351.

Thomas, J., Joseph, S., Thrivikramji, K.P., 2018. Estimation of soil erosion in a rain shadow river basin in the southern Western Ghats, India using RUSLE and transport limited sediment delivery function. Int. Soil Water Conserv. Res. 6 (2), 111–122.

Tong, Y., Bu, X., Chen, J., Zhou, F., Chen, L., Liu, M., Tan, X., Yu, T., Zhang, W., Mi, Z., Ma, L., Wang, X., Ni, J., 2017. Estimation of nutrient discharge from the Yangtze River to the East China Sea and the identification of nutrient sources. J. Hazard. Mater. 321, 728–736.

Torrence, C., Compo, G.P., 1998. A practical guide to wavelet analysis. Bull. Am. Meteorol. Soc. 79 https://doi.org/10.1175/1520-0477(1998)079<0061:APGTWA>2.0.CO;2.

van der Knijff, J.M., Jones, R.J.A., Montanarella, L., 2000. Soil Erosion Risk Assessment in Europe. Office for Official Publications of the European Communities, Luxembourg.

Wang, X., Hao, F., Cheng, H., Yang, S., Zhang, X., Bu, Q., 2011. Estimating non-point source pollutant loads for the large-scale basin of the Yangtze River in China. Environ. Earth Sci. 63 (5), 1079–1092.

Wang, W., Liu, X., Wang, Y., Guo, X., Lu, S., 2016. Analysis of point source pollution and water environmental quality variation trends in the Nansi Lake basin from 2002 to 2012. Environ. Sci. Pollut. Res. 23 (5), 4886–4897.

Wang, R., Min, J.u., Kronzucker, H.J., Li, Y., Shi, W., 2019b. N and P runoff losses in China's vegetable production systems: Loss characteristics, impact, and management practices. Sci. Total Environ. 663, 971–979.

Wang, D., Shao, J., Wang, J., Li, Y., Ni, J., Gao, M., Xie, D., 2015a. Estimation of sediment delivery ratio and modelling of absorbed nitrogen and phosphorus load in Three Gorges Reservoir Area nearly 20 years. Nongye Gongcheng Xuebao/Trans. Chinese Soc. Agric. Eng. 31, 167–176. https://doi.org/10.11975/j.issn.1002-6819.2015.15.023.

Wang, G., Wang, W., Luo, J., Zhang, Y., 2019a. Assessment of three types of shallow geothermal resources and ground-source heat-pump applications in provincial capitals in the Yangtze River Basin, China. Renew. Sustain. Energy Rev. 111, 392–421. https://doi.org/10.1016/j.rser.2019.05.029.

Wang, A.i., Yang, D., Tang, L., 2020. Spatiotemporal variation in nitrogen loads and their impacts on river water quality in the upper Yangtze River basin. J. Hydrol. (Amst) 590, 125487.

Wang, J., Zhu, B.o., Zhang, J., Müller, C., Cai, Z., 2015b. Mechanisms of soil N dynamics following long-term application of organic fertilizers to subtropical rain-fed purple soil in China. Soil Biol. Biochem. 91, 222–231.
Wischmeier, W.H. and, Smith, D.D., 1978. Predicting rainfall erosion losses-a guide to conservation planning. United States Department of Agriculture (USAD), a guide to conservation planning.
Wu, L., Long, T.-y., Liu, X., Mmereki, D., 2012. Simulation of soil loss processes based on rainfall runoff and the time factor of governance in the Jialing River Watershed, China. Environ. Monit. Assess. 184 (6), 3731–3748.
Wu, L., Long, T.-y., Liu, X., Ma, X.-y., 2013. Modeling impacts of sediment delivery ratio and land management on adsorbed non-point source nitrogen and phosphorus load in a mountainous basin of the Three Gorges reservoir area, China. Environ. Earth Sci. 70 (3), 1405–1422.
Xi, J., Li, Y., Liu, M., Wang, R.Z., 2017. Study on the thermal effect of the ground heat exchanger of GSHP in the eastern China area. Energy 141, 56–65.
Xiong, Y., Xu, W., Lu, N., Huang, S., Wu, C., Wang, L., Dai, F., Kou, W., 2021. Assessment of spatial–temporal changes of ecological environment quality based on RSEI and GEE: a case study in Erhai Lake Basin, Yunnan province, China. Ecol. Indic. 125, 107518.
Xu, K., Milliman, J.D., 2009. Seasonal variations of sediment discharge from the Yangtze River before and after impoundment of the Three Gorges Dam. Geomorphology 104 (3-4), 276–283.
Yan, B., Lu, Z., Li, J., Huo, J., 2021. Analysis of runoff characteristics in dry season at datong station on the mainstream of the Yangtze River. IOP Conf. Ser.: Earth Environ. Sci. 768 (1), 012066.
Yang, Y., Gao, B., Hao, H., Zhou, H., Lu, J., 2017. Nitrogen and phosphorus in sediments in China: a national-scale assessment and review. Sci. Total Environ. 576, 840–849.
Yang, D., Kanae, S., Oki, T., Koike, T., Musiake, K., 2003. Global potential soil erosion with reference to land use and climate changes. Hydrol. Process. 17 (14), 2913–2928.
Yang, H.F., Yang, S.L., Xu, K.H., Milliman, J.D., Wang, H., Yang, Z., Chen, Z., Zhang, C. Y., 2018. Human impacts on sediment in the Yangtze River: A review and new perspectives. Glob Planet Change 162, 8–17.
Yang, S.L., Zhang, J., Zhu, J., Smith, J.P., Dai, S.B., Gao, A., Li, P., 2005. Impact of dams on Yangtze River sediment supply to the sea and delta intertidal wetland response. J. Geophys. Res. Earth Surf. 110 https://doi.org/10.1029/2004JF000271.
Zhang, B., Ding, W., Xu, B.o., Wang, L., Li, Y.u., Zhang, C., 2020a. Spatial characteristics of total phosphorus loads from different sources in the Lancang River Basin. Sci. Total Environ. 722, 137863.
Zhang, H., Kang, M., Shen, L., Wu, J., Li, J., Du, H., Wang, C., Yang, H., Zhou, Q., Liu, Z., Gorfine, H., Wei, Q., 2020b. Rapid change in Yangtze fisheries and its implications for global freshwater ecosystem management. Fish Fish. 21, 601–620. https://doi.org/10.1111/faf.12449.
Zhang, Y., Wu, H., Yao, M., Zhou, J., Wu, K., Hu, M., Shen, H., Chen, D., 2021. Estimation of nitrogen runoff loss from croplands in the Yangtze River Basin: A meta-analysis. Environ. Pollut. 272, 116001.
Zhang, Q., Xu, C.-y., Becker, S., Jiang, T., 2006. Sediment and runoff changes in the Yangtze River basin during past 50 years. J. Hydrol. (Amst) 331 (3-4), 511–523.
Zhang, J., Zhang, Z.F., Liu, S.M., Wu, Y., Xiong, H., Chen, H.T., 1999. Human impacts on the large world rivers: Would the Changjiang (Yangtze River) be an illustration? Global Biogeochem. Cycles 13 (4), 1099–1105.
Zhao, S., Chen, Y., Gu, X., Zheng, M., Fan, Z., Luo, D., Luo, K., Liu, B., 2022. Spatiotemporal variation characteristics of livestock manure nutrient in the soil environment of the Yangtze River Delta from 1980 to 2018. Sci. Rep. 12 https://doi.org/10.1038/s41598-022-11267-9.
Zhiliang, S., Qun, L., Shumei, Z., Hui, M., Ping, Z., 2003. A nitrogen budget of the Changjiang River catchment. AMBIO: J. Human Environ. 32 https://doi.org/10.1639/0044-7447(2003)032[0065: anbotc]2 .0.co;2.
Zhong, Y., Lin, A., He, L., Zhou, Z., Yuan, M., 2020. Spatiotemporal dynamics and driving forces of urban land-use expansion: A case study of the Yangtze River Economic Belt, China. Remote Sens. (Basel) 12 (2), 287.
Zhou, M.-J., Shen, Z.-L., Yu, R.-C., 2008. Responses of a coastal phytoplankton community to increased nutrient input from the Changjiang (Yangtze) River. Cont. Shelf Res. 28 (12), 1483–1489.

Further reading

Peng, S., Ding, Y., Wen, Z., Chen, Y., Cao, Y., Ren, J., 2017. Spatiotemporal change and trend analysis of potential evapotranspiration over the Loess Plateau of China during 2011–2100. Agric. For. Meteorol. 233, 183–194.
Peng, S., Gang, C., Cao, Y., Chen, Y., 2018. Assessment of climate change trends over the Loess Plateau in China from 1901 to 2100. Int. J. Climatol. 38 (5), 2250–2264.